Power corrections to event shapes with mass-dependent operators

Vicent Mateu, Iain W. Stewart, and Jesse Thaler

Power Corrections to Event Shapes with Mass-Dependent Operators

Vicent Mateu,[1, 2] Iain W. Stewart,[1] and Jesse Thaler[1]

[1] *Center for Theoretical Physics, Massachusetts Institute of Technology, Cambridge, MA 02139, USA*
[2] *IFIC, UVEG - CSIC, Apartado de Correos 22085, E-46071, Valencia, Spain*

We introduce an operator depending on the "transverse velocity" r that describes the effect of hadron masses on the leading $1/Q$ power correction to event-shape observables. Here, Q is the scale of the hard collision. This work builds on earlier studies of mass effects by Salam and Wicke [1] and of operators by Lee and Sterman [2]. Despite the fact that different event shapes have different hadron mass dependence, we provide a simple method to identify universality classes of event shapes whose power corrections depend on a common nonperturbative parameter. We also develop an operator basis to show that at a fixed value of Q, the power corrections for many classic observables can be determined by two independent nonperturbative matrix elements at the 10% level. We compute the anomalous dimension of the transverse velocity operator, which is multiplicative in r and causes the power correction to exhibit non-trivial dependence on Q. The existence of universality classes and the relevance of anomalous dimensions are reproduced by the hadronization models in Pythia 8 and Herwig++, though the two programs differ in the values of their low-energy matrix elements.

I. INTRODUCTION

Event shapes have played a key role in establishing the structure of quantum chromodynamics (QCD). Indeed, the jet-like behavior of QCD collisions at high energies was established in 1975 by measuring the event shape sphericity in e^+e^- collisions [3]. Event shapes are used for precision determinations of the strong coupling constant α_s using e^+e^- data [4], and the same event shapes are used to tune Monte Carlo hadronization models to help make particle-level predictions for the Large Hadron Collider (LHC) (see e.g. Ref. [5]). Recently there has also been a resurgence of interest in event shapes because they are closely related to jet shapes, which are a sensitive probe of jet substructure [6, 7].

Event shapes require both perturbative and nonperturbative contributions from QCD. Therefore power corrections are an important theoretical ingredient for making event shape predictions. In the kinematic tail region, the leading nonperturbative effect is simply to shift perturbative event shape distributions by an amount suppressed by $1/Q$ [8]. Such $1/Q^n$ effects are known as power corrections, where Q is the scale of the hard collision. Some power corrections are known to exhibit universality, in the sense that the same nonperturbative shift parameter describes more than one event shape. Power corrections also encode the effect of hadron masses on event shape distributions [1], since different methods for treating the energy/momentum of soft hadrons with mass m_H can change event shapes by $\mathcal{O}(m_H/Q)$.

In this paper, we revisit the theoretical underpinnings of power corrections for e^+e^- event shapes, with a particular focus on universality and hadron masses. Building on the work of Salam and Wicke [1], we show that hadron mass effects break traditional power correction universality, but we are still able to define universality classes of event shapes with a common power correction. Building on the work of Lee and Sterman [2], we provide an operator definition of the leading power correction that demon-

strates that its hadron mass dependence is described by a "transverse velocity" distribution. Transverse velocity r is defined as

$$r \equiv \frac{p_\perp}{\sqrt{p_\perp^2 + m_H^2}}, \qquad (1)$$

where the transverse momentum $p_\perp$ is measured with respect to the thrust axis. The transverse velocity operator has nontrivial renormalization group evolution which is multiplicative in r, such that the leading power correction includes a term behaving as $(\alpha_s \ln Q)/Q$.

To put our work in context, it is worthwhile to review some of the key literature on event shapes and power corrections. Examples of classic e^+e^- dijet event shapes are thrust [9], the C-parameter [10, 11], hemisphere jet masses [12–14], jet broadening [15], and angularities [16], all of which were measured at LEP. The theoretical understanding of event shapes has undergone substantial progress in recent years, especially for perturbative calculations. Fixed-order corrections to event-shape distributions have been calculated up to $\mathcal{O}(\alpha_s^3)$ precision [17–23], and large singular logs have been resummed to N^{3}LL accuracy for thrust [24] and heavy jet mass [25], and to NLL for jet broadening [26–28]. For certain event shapes e, it can be demonstrated that the leading power correction parameter Ω_1^e appears both in the mean value of the event shapes as well as in the tail region of the full event shape distribution [8]. This fact was discussed using a factorization theorem for thrust in Ref. [29], and used to simultaneously extract $\alpha_s(m_Z)$ and Ω_1^τ from thrust data at N^{3}LL + $\mathcal{O}(\alpha_s^3)$ in Refs. [29, 30].

It is worth noting that heavy hadrons and heavy quark masses do not play a direct role in the $\mathcal{O}(m_H/Q)$ power corrections. Hadrons containing a heavy quark decay before reaching the detector, so m_H here refers to only light hadrons. At the partonic level it is straightforward to include the effect of heavy quark masses analytically [31–33]. Up to the one-loop level in the corresponding factorization theorem it is known that only the kine-

matic threshold and jet function are modified [34, 35], plus smaller contributions from non-singular terms [30].

To study nonperturbative power corrections, there have been two broad strategies. The first strategy is to build analytic models to describe the nonperturbative physics. For example, in the dispersive approach [36–38], one introduces an infrared cutoff μ_I below which the strong coupling constant is replaced by an effective coupling α_{eff}. Perturbative infrared effects coming from scales below the cutoff are subtracted, and nonperturbative effects are parametrized in terms of an average value for the effective coupling α_0 times μ_I.[1] The original dispersive approach relied on the single-gluon approximation. In Refs. [38, 45] the Milan factor was introduced as a refinement to handle multi-gluon diagrams. Another renormalon-inspired analytic model is provided in the dressed gluon approach [46–48].

A key prediction that emerged from these analytic models (first seen in the dispersive approach) was universality of power corrections [36, 40] (see also [44]). Universality posits that the leading power correction Ω_1^e to an event shape e can be separated into two pieces, a calculable coefficient c_e which depends on the event shape in question times a universal nonperturbative parameter Λ common to all event shape observables:

$$\Omega_1^e \to c_e \Lambda. \qquad (2)$$

Because of universality, one can extract the power correction Λ from one event shape measurement and apply it to another one, as studied in Refs. [2, 38, 45, 48–53].

The second strategy to understand power corrections is based on QCD factorization, where there is a formal separation of perturbative and nonperturbative contributions. The shape function was introduced in Refs. [52, 54] to describe nonperturbative corrections, and it accounts for a whole range of power corrections of the order $(\Lambda_{\text{QCD}}/eQ)^n$. In the tail region where $\Lambda_{\text{QCD}} \ll Q\,e \ll Q$, the shape function can be expanded in terms of derivatives of the Dirac delta function, and this translates into an operator expansion for the event-shape distribution. This shape function can be derived in the Collins-Soper-Sterman (CSS) approach to factorization [16, 52, 54–56]. The shape function also emerges naturally from factorization properties of Soft-Collinear Effective Theory (SCET) [57–61]. Here methods exist to systematically improve the description of the shape function [62, 63], and to sum large logs present in the subtractions needed to define the power corrections in a scheme that is free from the leading renormalon ambiguity [64, 65].

The key advantage of the factorization-based strategy is that one can express nonperturbative parameters in terms of matrix elements involving QCD fields. For example, the leading power correction Ω_1 can be expressed in terms of the energy flow operator [2, 66–68]. Using this fact, Lee and Sterman [2] rigorously derived universality for the leading power correction without relying on an analytic model. This proof of power correction universality solely uses QCD first principles.

The drawback of both of the two above strategies is that they start by making the assumption that all final state hadrons can be considered to be massless. (An important exception to this is Ref. [39, 43], where mass effects were studied with renormalons using massive gluons.) The massless assumption is certainly valid at the parton level, but the actual hadrons measured in an event shape are of course massive. One might erroneously argue that at very high energies the hadron masses can be safely neglected, but because nonperturbative effects are caused by soft particles whose momenta are of order $\Lambda_{\text{QCD}} \sim m_H$, their masses contribute at order m_H/Q, which is the same order as the leading power correction. One could try to study the effect of hadron masses by using Monte Carlo hadronization models, but this approach is not fully satisfactory since there is no clean separation between perturbative parton shower evolution and nonperturbative hadronization effects, and there is no guarantee that one can systematically improve the accuracy of the treatment of hadronization effects.

The first serious study of hadron mass effects on power corrections was performed by Salam and Wicke [1], where they argued that universality does not hold for event shapes such as thrust, jet masses, or the C-parameter with their traditional definitions. However, they showed that universality can be restored if one makes measurements in the E-scheme, where one performs the following substitution in the event shape definition:

$$\vec{p}_i \to \frac{E_i}{|\vec{p}_i|}\,\vec{p}_i\,. \qquad (3)$$

Ref. [1] also argues that hadron mass effects, in addition to breaking universality, generate a power correction of the form $(\ln Q)^A/Q$, with $A \sim 1.5$.

In this paper we will devise a rigorous operator-based method of treating hadron mass effects in the leading event shape power correction by defining a transverse velocity operator. We generalize Ω_1^e to a function $\Omega_1(r, \mu)$ which accounts for both the transverse velocity dependence through r as well as renormalization group evolution through μ. Using this operator we derive universality classes for event shapes in the presence of hadron masses, following the treatment of Ref. [2], and show that each event shape belongs to a unique class. From studying the r- and μ-dependence, we will largely confirm the results of Salam and Wicke.

---

[1] The dispersive approach was motivated by the study of renormalons (see Ref. [39] for a review). Renormalons refer to an ambiguity in a resummed perturbative series of order $(\Lambda/Q)^p$, and this ambiguity is related to the nonperturbative power correction. Renormalon-based models were originally applied to the mean values of the event-shape distributions [36, 40–42] (see also [43]) and later generalized to the dijet limit of distributions as well [8, 44].

Thrust [9][2]:	$\tau = \dfrac{1}{Q_p} \min_{\hat{t}} \sum_i \left(|\vec{p}_i| - |\vec{p}_i \cdot \hat{t}| \right) ,$		$\bar{\tau} = \dfrac{Q_p \tau}{Q} = \dfrac{1}{Q} \sum_i p_i^\perp e^{-|\eta_i|} ,$
2-jettiness [69]:	$\tau_2 = \dfrac{1}{Q} \min_{\hat{t}} \sum_i \left(E_i - |\vec{p}_i \cdot \hat{t}| \right) ,$		$\bar{\tau}_2 = \tau_2 = \dfrac{1}{Q} \sum_i m_i^\perp e^{-|y_i|} .$
Angularities [16][3]:	$\tau_{(a)} = \dfrac{1}{Q} \sum_i E_i \, (\sin \theta_i)^a (1 - |\cos \theta_i|)^{1-a} ,$		$\bar{\tau}_{(a)} = \tau_{(a)} = \dfrac{1}{Q} \sum_i p_i^\perp \dfrac{E_i}{|\vec{p}_i|} \, e^{-|\eta_i|(1-a)} ,$
C-parameter [10, 11][4]:	$C = \dfrac{3}{2Q_p^2} \sum_{i,j} |\vec{p}_i||\vec{p}_j| \sin^2 \theta_{ij} ,$		$\bar{C} = \dfrac{3}{Q} \sum_i \dfrac{p_i^\perp}{\cosh(\eta_i)} ,$
Jet Masses [12–14]:	$\rho_\pm = \dfrac{1}{Q^2} \left(\sum_{i \in \pm} p_i^\mu \right)^2 ,$		$\bar{\rho}_\pm = \dfrac{1}{Q} \sum_i m_i^\perp \theta(\pm y_i) \, e^{\mp y_i} ,$

TABLE I. Examples of event shapes e with their original definitions, as well as formulae $\bar{e}$ that are valid for $e \ll e_{\max}$. See the text below Eq. (7) for a further description of the notation.

The remainder of this paper is organized as follows. In Sec. II, we set the notation for event shapes and power corrections. In Sec. III, we introduce the transverse velocity operator whose matrix elements yield the leading power correction. We explore the consequences of universality classes in Sec. IV, and use a complete operator basis to derive approximate universality relations. We consider the effect of renormalization group evolution in Sec. V, where we derive the anomalous dimension for $\Omega_1(r,\mu)$ and compare to the hadronization models of Pythia 8 and Herwig++. We conclude in Sec. VI with a discussion of the implications and extensions of our results, in particular for the LHC.

II. POWER CORRECTIONS FOR DIJET EVENT SHAPES

We begin by reviewing the notation for kinematics and event shapes in Sec. II A, various hadron mass schemes in Sec. II B, and the basics of how power corrections impact event shapes in Sec. II C. Readers familiar with these topics can skip to Sec. III, where we introduce the transverse velocity operator.

A. Event Shapes with Transverse Velocity

A dimensionless event shape e is an observable defined on final-state particles which can be used to describe the

jet-like structure of an event. To describe particle momenta, we use rapidity y, pseudo-rapidity η, transverse momenta $p_\perp = |\vec{p}_\perp|$, and transverse mass $m^\perp$, where $m_\perp = \sqrt{p_\perp^2 + m^2}$ for a particle of mass m. Defining rapidities and transverse momenta relative to the $\hat{z}$ axis, a 4-momentum $p^\mu = (E, \vec{p})$ can be written in two equivalent forms as

$$p^\mu = \left(m_\perp \cosh y, \vec{p}_\perp, m_\perp \sinh y \right) \qquad (4)$$
$$= \left(\sqrt{m^2 + p_\perp^2 \cosh^2 \eta}, \vec{p}_\perp, p_\perp \sinh \eta \right) .$$

In terms of the polar angle θ from the $\hat{z}$ axis, $\eta = -\ln \tan(\theta/2)$. The standard velocity of a relativistic particle is $v = |\vec{p}|/E$. In our analysis, an important role will be played by the "transverse velocity" r defined by

$$r = \frac{p_\perp}{m_\perp} = \frac{p_\perp}{\sqrt{p_\perp^2 + m^2}} . \qquad (5)$$

In general, the pseudo-rapidity and velocity of a particle can be expressed in terms of r and y:

$$\eta = \eta(r,y) = \ln \left(\frac{\sqrt{r^2 + \sinh^2 y} + \sinh y}{r} \right) , \qquad (6)$$
$$v = v(r,y) = \frac{\sqrt{r^2 + \sinh^2 y}}{\cosh y} .$$

For massless particles, $r = v = 1$ and $\eta = y$.

Our focus will be on dijet event shapes in $e^+ e^-$ collisions, which have the property that $e \to 0$ implies back-to-back pencil-like jets (and $e = 0$ for the lowest order partonic configuration $e^+ e^- \to q\bar{q}$). To maintain simplicity, we will not include recoil sensitive observables such as broadening [72] in our analysis.[5] The event shapes

---

[2] The original thrust variable is $T = 1 - \tau$.

[3] For $a = 1$, angularities reduce to jet broadening and hence are recoil sensitive. Throughout this paper we assume that $a < 1$ by an amount that allows recoil effects to be neglected.

[4] The shape parameter H_2 introduced in [70, 71] is equivalent to the C-parameter with the substitution $Q \to Q_p$.

[5] For a recoil sensitive observable, the axis used to compute e (typically the thrust axis $\hat{t}$) differs from the axis which minimizes e by an amount that can have an $\mathcal{O}(1)$ effect on the value of e.

$f_e(r,y)$	τ	τ_2	$\tau_{(a)}$	C	$\rho_\pm$
Original	$r\,e^{-|\eta|}$	$e^{-|y|}$	$\dfrac{r}{v}\,e^{-|\eta|(1-a)}$	$\dfrac{3\,r}{\cosh\eta}$	$\theta(\pm y)\,e^{\mp y}$
P-scheme	$r\,e^{-|\eta|}$	$r\,e^{-|\eta|}$	$r\,e^{-|\eta|(1-a)}$	$\dfrac{3\,r}{\cosh\eta}$	$r\,\theta(\pm\eta)\,e^{\mp\eta}$
E-scheme	$\dfrac{r}{v}\,e^{-|\eta|}$	$\dfrac{r}{v}\,e^{-|\eta|}$	$\dfrac{r}{v}\,e^{-|\eta|(1-a)}$	$\dfrac{r}{v}\dfrac{3}{\cosh\eta}$	$\dfrac{r}{v}\,\theta(\pm\eta)\,e^{\mp\eta}$
R-scheme	$r\,e^{-|y|}$	$r\,e^{-|y|}$	$r\,e^{-|y|(1-a)}$	$\dfrac{3\,r}{\cosh y}$	$r\,\theta(\pm y)\,e^{\mp y}$
J-scheme	$e^{-|y|}$	$e^{-|y|}$	$e^{-|y|(1-a)}$	$\dfrac{3}{\cosh y}$	$\theta(\pm y)\,e^{\mp y}$

TABLE II. The functions $f_e(r,y)$ of "transverse velocity" r and rapidity y for various dijet event shapes using several different schemes for treating hadron mass effects. Here $\eta = \eta(r,y)$ and $v = v(r,y)$ are given in Eq. (6).

we consider are also bounded as $0 \le e \le e_{\max}$, where the maximum value $e_{\max}$ depends on the observable in question but is typically $\mathcal{O}(1)$. For the $e \ll e_{\max}$ limit, one can sometimes simplify the expression defining e by neglecting corrections of $\mathcal{O}(e^2)$. We will distinguish expressions for event shapes that are valid under this approximation by adding a bar, $\bar{e}$.

Various examples of dijet event shapes are shown in Tab. I, including their original definitions e and expressions $\bar{e}$ valid when $e \ll e_{\max}$. For angularities and 2-jettiness, there are no simplifications in the dijet limit, so $\bar{e} = e$ without higher order terms. The notation for various items in the table require explanation. The normalization factors are defined by

$$Q_p = \sum_i |\vec{p}_i|\,, \qquad Q = \sum_i E_i\,. \qquad (7)$$

The unit vector $\hat{t}$ obtained in the minimization defining thrust τ is referred to as the thrust axis, and we have taken it to be aligned with $\hat{z}$ to define rapidities. The angle between particles i and j is denoted by θ_{ij}, and the angle between particle i and $\hat{t}$ is denoted by θ_i. Finally, the $\pm$ labels refer to each of the two hemispheres defined by the plane normal to the thrust axis. For later convenience, we have written all $\bar{e}$ formulae in terms of $p_\perp$, $m_\perp$, y, and/or η. Note that we can always replace $Q_p \to Q$ in the overall normalization for $\bar{e}$, since the correction in doing so is beyond the order we are working.

For a dijet event shape e, the largest part of the cross section comes from $e \ll e_{\max}$, as do the most important hadronization corrections which are the focus of this paper. The simplicity of the dijet limit makes it possible to derive factorization theorems[6] for these cross sections which facilitate calculations of higher order perturbative

corrections $\propto \alpha_s^j (\ln^k e)/e$, as well as defining nonperturbative corrections in terms of field-theoretic matrix elements. For our purposes, the relevant point is that at leading order in the nonperturbative corrections, we can split $\bar{e}$ into perturbative (e_{p}) and non-perturbative (e_Λ) contributions[7]

$$\bar{e} = e_{\mathrm{p}} + e_\Lambda\,. \qquad (8)$$

The e_{p} term is generated by particles with momenta $p \gg \Lambda_{\mathrm{QCD}}$ and here we can neglect corrections from hadron masses m_H up to second order in the m_H/Q expansion. The e_Λ term involves corrections from soft particles with momenta $p^\mu \sim \Lambda_{\mathrm{QCD}}$, and from Tab. I, we see that $e_\Lambda \sim \Lambda/Q$ where $\Lambda \sim m_H \sim \Lambda_{\mathrm{QCD}}$. Thus simple power counting dictates that to determine e_Λ, we cannot neglect hadron mass effects in the definition of $\bar{e}$.

For our analysis, we will find it convenient to characterize each event shape by a function $f_e(r,y)$ of the transverse velocity r and rapidity y, which we define from the $e \ll e_{\max}$ limit via

$$\bar{e} = \frac{1}{Q}\sum_i m_i^\perp f_e(r_i, y_i)\,. \qquad (9)$$

The various examples in Tab. I have the following $f_e(r,y)$ functions:

$$f_\tau(r,y) = \sqrt{r^2 + \sinh^2(y)} - \sinh|y|\,, \qquad (10)$$

$$f_{\tau_2}(r,y) = e^{-|y|}\,,$$

$$f_{\tau_{(a)}}(r,y) = r^a\,\frac{\partial\eta(r,y)}{\partial y}\left(\sqrt{r^2 + \sinh^2 y} - \sinh|y|\right)^{1-a}\,,$$

$$f_C(r,y) = \frac{3\,r^2}{\sqrt{r^2 + \sinh^2 y}}\,,$$

---

[6] The simplest examples of dijet factorization rely on being able to write the dijet event shape as a sum of contributions from energetic collinear particles in the $\pm$ hemispheres $(n, \bar{n})$, soft perturbative particles (s), and soft nonperturbative particles (Λ), via $\bar{e} = e_n + e_{\bar{n}} + e_s + e_\Lambda$. See for example Ref. [68].

[7] The heavy jet mass event shape $\rho_H = \max\{\rho_+, \rho_-\}$ does not admit such a decomposition, and correspondingly its factorization formula is a bit more complicated. The light jet mass $\rho_L = \min\{\rho_+, \rho_-\}$ is not a true dijet event shape since $\rho_L \to 0$ does not imply a dijet configuration.

$$f_{\rho_\pm}(r,y) = \theta(\pm y)\, e^{\mp y}\,,$$

where

$$\frac{E}{|\vec{p}|} = \frac{\cosh y}{\sqrt{r^2 + \sinh^2 y}} = \frac{\partial \eta(r,y)}{\partial y} = \frac{1}{v}\,. \qquad (11)$$

The translation from the notation of Ref. [1] (denoted with superscripts SW) to our notation is $f_e^{\text{SW}}(y, m^2/p_\perp^2) = f_e(r,y)/r$.

B. Hadron Mass Schemes

In experimental analyses, different "schemes" are often adopted for the treatment of hadron masses depending on the available information. In the context of event shapes, a detailed discussion of these schemes is given in Ref. [1]. These schemes correspond to different choices for $f_e(r,y)$ that yield the same value for the perturbative contribution e_{p} but potentially different values for the nonperturbative contribution e_Λ. The schemes considered in this paper are summarized in Tab. II.

In the "P-scheme", one makes measurements with only 3-momentum information. One performs the substitution $E_i \to |\vec{p}_i|$ in the formula for event shapes, and correspondingly $m_\perp \to r\, m_\perp$ in Eq. (9). To satisfy infrared safety, the original $f_e(r,y)$ must tend to a constant value (possibly zero) in the $r \to 0$ limit, and this implies that the P-scheme event shapes will always vanish linearly with r. The P-scheme replacement affects the jet masses, angularities, and 2-jettiness which become

$$\tau_2^P = \frac{1}{Q_p} \sum_i p_i^\perp e^{-|\eta_i|} = \tau\,, \qquad (12)$$

$$\tau_{(a)}^P = \frac{1}{Q_p} \sum_i |\vec{p}_i|\,(\sin\theta_i)^a (1 - |\cos\theta_i|)^{1-a}\,,$$

$$\rho_\pm^P = \frac{2}{Q_p^2} \sum_{(i,j)\in\pm} |\vec{p}_i||\vec{p}_j| \sin^2 \frac{\theta_{ij}}{2}\,.$$

Another scheme discussed in Ref. [1] is the "E-scheme" (see Refs. [44, 54, 66, 73] for earlier discussions), where only measurements of energies and angles are used to construct observables. Compared to the P-scheme, one makes the substitution

$$\vec{p}_i \to \frac{E_i}{|\vec{p}_i|}\,\vec{p}_i \qquad (13)$$

in the formula for event shapes. This modifies all examples in Tab. I except for angularities:

$$\tau^E = \tau_2^E = \frac{1}{Q} \sum_i E_i(1 - |\cos\theta_i|)\,, \qquad (14)$$

$$\rho_\pm^E = \frac{2}{Q^2} \sum_{(i,j)\in\pm} E_i E_j \sin^2 \frac{\theta_{ij}}{2}\,,$$

$$C^E = \frac{3}{2Q^2} \sum_{i,j} E_i E_j \sin^2 \theta_{ij}\,.$$

Note that thrust and 2-jettiness are identical in the E-scheme, $\tau_2^E = \tau^E$. In the P-scheme, the event shapes are all linear in r, and hence the corresponding E-scheme results for $f_e(r,y)$ are simply obtained by multiplying by $E/|\vec{p}| = 1/v$. Note that the E-scheme and P-scheme are defined in terms of pseudo-rapidity η (equivalently, the polar angle θ).

In order to consider a wider range of observables, we will introduce two new schemes. In the "R-scheme" (rapidity scheme), we take event shapes defined in the P-scheme and make the replacement $\eta \to y$. To define R-scheme event shapes where $\bar{e} \neq e$, we carry out this replacement for $\bar{e}$, and then define $e^R = \bar{e}^R$. The "J-scheme" is the closest to the jet mass observables, and is defined by taking the R-scheme result and setting $r = 1$, $f_{e^J}(r,y) = f_{e^R}(1,y)$.

We emphasize that the naming of schemes discussed here is set simply by convention. For understanding power corrections one only needs to know the functional form of $f_e(r,y)$.

C. Effect of Power Corrections on Cross Sections

For recoil-less dijet event shapes that satisfy Eq. (8), the perturbative/nonperturbative factorization of the differential distribution in the $e \to 0$ limit implies

$$\frac{d\sigma}{de} = \int d\ell\, \frac{d\hat{\sigma}}{de}\left(e - \frac{\ell}{Q}\right) F_e(\ell)\left[1 + \mathcal{O}(e)\right]. \qquad (15)$$

Here $d\hat{\sigma}/de$ is the most singular perturbative cross section to all orders in α_s, and contains the full leading power perturbative soft function. F_e is the shape function that depends on the specific event shape one is interested in. It contains nonperturbative power corrections (and, as we will see, perturbative corrections). If $Qe \sim \Lambda_{\text{QCD}}$, then the entire function $F_e(\ell)$ has an important impact on the cross section and in practice one models it with a few coefficients which can be fit to data [52, 54], or uses a complete basis which can be systematically improved [63].

For $Qe \gg \Lambda_{\text{QCD}}$, the function $F_e(\ell)$ can be expanded for $\ell \gg \Lambda_{\text{QCD}}$ in terms of nonperturbative matrix elements of operators. The first terms are

$$F_e(\ell) = \delta(\ell) - \delta'(\ell)\,\Omega_1^e + \mathcal{O}\!\left(\frac{\alpha_s \Lambda_{\text{QCD}}}{\ell}\right) + \mathcal{O}\!\left(\frac{\Lambda_{\text{QCD}}^2}{\ell^3}\right), \qquad (16)$$

where $\Omega_1^e(\mu)$ is a dimension-1 nonperturbative matrix element (defined here in the $\overline{\text{MS}}$ scheme) that encodes the power corrections we wish to study. It is defined by

$$\Omega_1^e = \langle 0 |\, \overline{Y}_{\bar{n}}^\dagger Y_n^\dagger (Q\hat{e}) Y_n \overline{Y}_{\bar{n}} \,| 0 \rangle\,, \qquad (17)$$

where $(Q\hat{e})$ is a Q-independent field-theoretic operator that measures the combination $Q\bar{e}$, and Y $(\overline{Y})$ are Wilson lines with gluon fields in the fundamental (anti-fundamental) color representation along the directions specified by $n = (1, \hat{t})$ and $\bar{n} = (1, -\hat{t})$. For example,

$$Y_n = \mathrm{P} \exp\left[ig \int_0^\infty \mathrm{d}s\, n \cdot A(ns) \right], \qquad (18)$$

where P stands for path-ordering and A^μ is the gluon field. The fact that the dimension-1 matrix element Ω_1^e is nonperturbative is easy to understand on dimensional grounds since the only scale for this QCD vacuum matrix element is Λ_{QCD}. In Eq. (16) the $\mathcal{O}(\alpha_s \Lambda_{\mathrm{QCD}}/\ell)$ term involves perturbative corrections to the leading power correction which will be discussed in Sec. V B.

Plugging Eq. (16) into Eq. (15) for the event shape distribution one finds

$$\frac{\mathrm{d}\sigma}{\mathrm{d}e} = \frac{\mathrm{d}\hat{\sigma}}{\mathrm{d}e} - \frac{\Omega_1^e}{Q} \frac{\mathrm{d}}{\mathrm{d}e} \frac{\mathrm{d}\hat{\sigma}}{\mathrm{d}e} + \dots, \qquad (19)$$

where the ellipses denotes higher order terms in α_s and $\Lambda_{\mathrm{QCD}}/\ell$. Eq. (19) corresponds to a shift $e \to e - \Omega_1^e/Q$ to first order in $1/Q$, and reproduces the known shift found in the dispersive approach [36–38]. Thus, the dominant effect of power corrections (hadronization) on dijet event shapes for $Qe \gg \Lambda_{\mathrm{QCD}}$ is simply a shift in the distribution.

Following Ref. [30] we note that as long as $\mathrm{d}\hat{\sigma}/\mathrm{d}e$ tends to zero in the far tail region, one can derive an operator product expansion for the first moment of the distribution as well. Defining the full and perturbative moments as

$$\langle e \rangle \equiv \int \mathrm{d}e\, e\, \frac{1}{\sigma}\frac{\mathrm{d}\sigma}{\mathrm{d}e}, \qquad \langle e \rangle_{\mathrm{pert}} \equiv \int \mathrm{d}e\, e\, \frac{1}{\hat{\sigma}}\frac{\mathrm{d}\hat{\sigma}}{\mathrm{d}e}, \quad (20)$$

one can use the factorization in Eq. (15) and the expansion of the shape function in Eq. (16) to show

$$\langle e \rangle = \langle e \rangle_{\mathrm{pert}} + \frac{\Omega_1^e}{Q} + \dots, \qquad (21)$$

where again the ellipses denote higher order terms. For the event shapes in Tab. I, all the event shapes except for C tend to zero in the far tail region, so the leading power correction generates a Q-dependent shift of their first moment. We will use this feature to extract Ω_1^e from the Pythia 8 and Herwig++ hadronization models in Sec. V D. See Ref. [52] for a discussion of the modification necessary for the C-parameter moment.

III. THE TRANSVERSE VELOCITY OPERATOR

The goal of this paper is to study the effect of hadron masses on the power correction in Eq. (17). In order to formulate the operator $(Q\hat{e})$ appearing in the definition of

Ω_1^e, we will follow the energy-momentum tensor approach of Refs. [2, 68], and generalize it so that we can treat the dependence on the transverse velocity r. In particular, the event shape e will be written as the eigenvalue of an operator acting on the final state which includes hadron mass effects. In Sec. III B, we consider the crucial role of boost invariance for identifying universality classes.

A. Comparison to Transverse Energy Flow

To set up our analysis, it will be convenient to first review definitions from the literature that do not account for hadron mass effects in the event shapes. These correspond to setting $r = 1$ for the event shapes defined by Eq. (9). The transverse energy flow operator $\hat{\mathcal{E}}_T(\eta)$ is defined by [2]

$$\hat{\mathcal{E}}_T(\eta)|X\rangle = \sum_{i \in X} p_i^\perp\, \delta(\eta - \eta_i)|X\rangle. \qquad (22)$$

(Here and below we suppress the dependence on the thrust axis $\hat{t}$.) The operator $\hat{\mathcal{E}}_T(\eta)$ is related to the energy-momentum tensor $T^{\mu\nu}(t, \vec{x})$ by [66–68, 74]

$$\hat{\mathcal{E}}_T(\eta) = \frac{1}{\cosh^3\eta} \int_0^{2\pi}\mathrm{d}\phi \lim_{R\to\infty} R^2 \int_0^\infty \mathrm{d}t\, \hat{n}_i\, T^{0i}(t, R\,\hat{n}), \quad (23)$$

where $\hat{n}$ is a unit vector pointing in the (θ, ϕ) direction for the θ corresponding to η.[8] Using $\hat{\mathcal{E}}_T(\eta)$, we can define an operator for the event shape $\bar{e}$ by [2]

$$\hat{e}_0|X\rangle \equiv \frac{1}{Q} \int \mathrm{d}\eta\, f_e(\eta)\, \hat{\mathcal{E}}_T(\eta)|X\rangle, \qquad (24)$$

where in the notation defined in Eq. (9), this $f_e(\eta) = f_e(r = 1, y = \eta)$. For massless particles with $r = 1$, this operator satisfies $\hat{e}_0|X\rangle = \bar{e}(X)|X\rangle$, so the measurement operator in Eq. (17) is given by $\widehat{\mathcal{M}}_e = Q\hat{e}_0$.

To generalize this operator formalism to include hadron masses, we require a transverse momentum flow operator that is more differential, namely a $\hat{\mathcal{E}}_T(r, y)$ which can pick out states that have a particular transverse velocity r. We will refer to this simply as the "transverse velocity operator", and define it by its action on a state

$$\hat{\mathcal{E}}_T(r, y)|X\rangle = \sum_{i \in X} m_i^\perp \delta(r - r_i)\, \delta(y - y_i)\,|X\rangle. \qquad (25)$$

---

[8] In the proof of Ref. [68] that Eq. (23) reproduces Eq. (22) for scalars and fermions, one assumes that all particles are massless. If the energy momentum tensor is considered for massive fields, then Eq. (23) yields Eq. (22), but η must be identified with pseudo-rapidity and the factor $p_i^\perp \to m_i^\perp$.
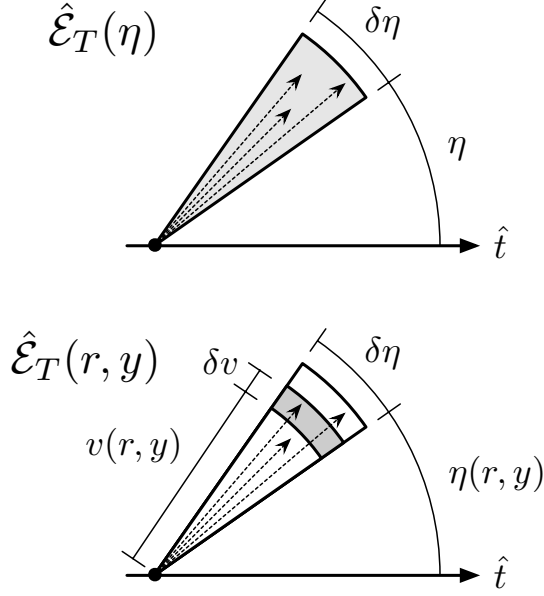
FIG. 1. The energy flow operator (top) compared to the transverse velocity operator (bottom). Measurements are made with respect to the thrust axis $\hat{t}$. The dashed arrows correspond to particles with lengths given by the particle velocities. Shading indicates which particles are measured by the operator. Note that the velocity $v(r, y)$ and pseudo-rapidity $\eta(r, y)$ are functions of the transverse velocity r and rapidity y.

Note that here we use rapidity y rather than pseudo-rapidity η. In App. A we show that $\hat{\mathcal{E}}_T(r, y)$ can be defined in terms of the energy-momentum tensor as

$$\hat{\mathcal{E}}_T(r, y) = \frac{r \operatorname{sech}^4 y}{\sqrt{r^2 + \sinh^2 y}} \lim_{R \to \infty} R^3 \int_0^{2\pi} d\phi\, \hat{n}_i\, T^{0i}(R, R\, v\, \hat{n}), \tag{26}$$

where $v = v(r, y)$ and $\eta = \eta(r, y)$ are given in Eq. (6). The unit vector $\hat{n}$ again points in the (θ, ϕ) direction and hence depends on y and r through its dependence on $\eta = -\ln \tan(\theta/2)$.

The physical picture for the distinction between $\hat{\mathcal{E}}_T(\eta)$ and $\hat{\mathcal{E}}_T(r, y)$ is shown in Fig. 1. The energy flow operator $\hat{\mathcal{E}}_T(\eta)$ involves an expanding sphere of radius R integrated over all time, and measures the total transverse momentum for rapidities in an infinitesimal interval $\delta\eta$ about η. The transverse velocity operator $\hat{\mathcal{E}}_T(r, y)$ involves a spheroid that expands in both space and time with a finite velocity v, and it measures the total transverse mass for particles in an infinitesimal interval in both η and the velocity v (or equivalently an infinitesimal interval in y and r). Using $\hat{\mathcal{E}}_T(r, y)$, the value of an event shape $\bar{e}$ for a state $|X\rangle$ with massive or massless particles

is given by $\hat{e}|X\rangle = \bar{e}(X)|X\rangle$ where the operator

$$\hat{e} \equiv \frac{1}{Q} \int_{-\infty}^{+\infty} dy \int_0^1 dr\, f_e(r, y)\, \hat{\mathcal{E}}_T(r, y) \tag{27}$$

involves $f_e(r, y)$ defined in Eq. (9). This is the desired generalization of Eq. (24) that will allow us to treat the effect of hadron masses on event shape power corrections. The result in Eq. (27) completes the matrix element definition of Ω_1^e given in Eq. (17).

B. Boost Invariance

Both $\hat{\mathcal{E}}_T(\eta)$ and $\hat{\mathcal{E}}_T(r, y)$ have nice transformation properties under longitudinal boosts. These arguments were first given in Ref. [2] in the context of $\hat{\mathcal{E}}_T(\eta)$ to prove universality of power corrections for massless particles, and we will extend the logic for $\hat{\mathcal{E}}_T(r, y)$ to develop the notion of universality classes which account for hadron masses in the next section.

For the case of massless particles in Ref. [2], $\eta = y$ and it was shown that under a boost of rapidity y' along the thrust-axis:

$$U(y')\hat{\mathcal{E}}_T(y)U(y')^\dagger = \hat{\mathcal{E}}_T(y + y'). \tag{28}$$

Due to the invariance of the vacuum $|0\rangle$ and Wilson lines Y_n and $Y_{\bar{n}}$ under this boost, we can choose $y' = -y$ so

$$\langle 0 | \overline{Y}_{\bar{n}}^\dagger Y_n^\dagger \mathcal{E}_T(y) Y_n \overline{Y}_{\bar{n}} | 0 \rangle = \langle 0 | \overline{Y}_{\bar{n}}^\dagger Y_n^\dagger \mathcal{E}_T(0) Y_n \overline{Y}_{\bar{n}} | 0 \rangle. \tag{29}$$

Using Eq. (24), again with $\eta = y$, the power correction in Eq. (17) simplifies to

$$\left[\int_{-\infty}^{+\infty} d\eta\, f_e(\eta) \right] \langle 0 | \overline{Y}_{\bar{n}}^\dagger Y_n^\dagger \mathcal{E}_T(0) Y_n \overline{Y}_{\bar{n}} | 0 \rangle. \tag{30}$$

Thus as argued in Ref. [2], the power correction is universal if one neglects hadron mass effects, since it depends on a common nonperturbative matrix element times a calculable η integral specific to an event shape. This result agrees with the the dispersive approach [36–38], and also explains why it only applies for the first power correction in the expansion of Eq. (16).

We can apply the same logic to our transverse velocity operator in Eq. (25), now accounting for the effect of hadron masses. Under a boost of rapidity y',

$$U(y')\, \hat{\mathcal{E}}_T(r, y)\, U(y')^\dagger = \hat{\mathcal{E}}_T(r, y + y'). \tag{31}$$

Choosing $y' = -y$, we find that the leading power corrections to dijet event shapes are all described by the nonperturbative matrix element

$$\Omega_1(r) \equiv \langle 0 | \overline{Y}_{\bar{n}}^\dagger Y_n^\dagger \hat{\mathcal{E}}_T(r, 0) Y_n \overline{Y}_{\bar{n}} | 0 \rangle \tag{32}$$

which depends only on r and is independent of the event shape e. Using Eq. (27), the power correction Ω_1^e simplifies to

$$\Omega_1^e = \int_0^1 dr \left[\int_{-\infty}^{+\infty} dy\, f_e(r,y) \right] \Omega_1(r) . \qquad (33)$$

We will consider the implications of Eqs. (32) and (33) for universality in the next section. Note that there is no limit where Eq. (33) approaches the massless approximation in Eq. (30).

IV. UNIVERSALITY FOR EVENT SHAPES

A. Universality Classes Defined by $g(r)$

The boost invariance logic of the previous section shows that for the power correction Ω_1^e, we can factor out the rapidity dependence from the nonperturbative matrix element. We define the integral appearing in Eq. (33) as

$$\int_{-\infty}^{+\infty} dy\, f_e(r,y) \equiv c_e\, g_e(r) , \qquad (34)$$

where $g_e(1) = 1$ and

$$c_e = \int_{-\infty}^{+\infty} dy\, f_e(1,y) , \quad g_e(r) = \frac{1}{c_e} \int_{-\infty}^{+\infty} dy\, f_e(r,y) . \qquad (35)$$

(For the special case of event shapes that vanish for massless partons, $\int dy\, f_e(1,y) = 0$, we define $c_e = 1$ and let $g_e(1) = 0$.) Thus, the leading power correction for an event shape e can be written as

$$\Omega_1^e = c_e\, \Omega_1^{g_e} , \qquad \Omega_1^{g_e} \equiv \int_0^1 dr\, g_e(r)\, \Omega_1(r) , \qquad (36)$$

where $\Omega_1(r)$ is given in Eq. (32).

Using the fact that for massless hadrons $f_e(\eta) = f_e(r = 1, y = \eta)$ in Eq. (30), we see that the coefficients c_e are precisely the classic universality prefactors that one derives neglecting the hadron mass dependence of event shapes [2, 8, 36, 37, 44, 54, 74–76]. The function $g_e(r)$ then encodes the effect of hadron masses through the nonperturbative parameter $\Omega_1^{g_e}$.

The key result from Eq. (36) is that each unique function $g_e(r)$ defines a universality class for dijet events shapes. In particular, for two different event shape variables a and b, if $g_a(r) = g_b(r)$ then $\Omega_1^{g_a} = \Omega_1^{g_b}$ (equivalently $\Omega_1^a/c_a = \Omega_1^b/c_b$), so their power corrections agree up to the calculable constants c_a and c_b. We say that two such event shapes belong to the same universality class, and we will often refer to Ω_1^g as the universal power correction defined by $g(r)$.

Recall from Tab. I that the $f_e(r,y)$ functions in general depend on the measurement scheme used for treating hadron mass effects (E-scheme, P-scheme, etc). The

functions $g_e(r)$ will also in general vary with the measurement scheme. However, the c_e coefficients are independent of the scheme for treating hadron masses since they are defined with $r = 1$ corresponding to the massless limit, and $f_e(r = 1, y)$ is the same in all schemes. Our classification of universality classes with common $g(r)$'s is the same as the identification of event shapes that have the same hadron mass effects made in Ref. [1], and we will elaborate on the precise notational relationship in Sec. IV C below.

A summary of coefficients c_e, functions $g_e(r)$, and universality classes are collected in Tables III, IV, and V, and will be discussed in detail in Secs. IV B and IV C below. Since many of the standard event shapes have different $g(r)$ functions, their power corrections are not related by universality. We will take up the question of numerically approximate relations between power corrections in different universality classes in Sec. IV D. Finally in Sec. IV E we consider the impact of changing the renormalization scheme defining $\Omega_1(r)$ from $\overline{\text{MS}}$ to a renormalon-free scheme.

B. Generalized Angularities

In order to see how universality works in practice, it is instructive to consider a family of event shapes which are a simple generalization of angularities, and are labeled by two numbers $n \geq 0$ and $a < 1$:

$$\tau_{(n,a)} \equiv \sum_i m_i^\perp r_i^n e^{-|y_i|(1-a)} . \qquad (37)$$

This corresponds to extending the R-scheme definition of angularities by incorporating a positive power n of $r = p_\perp/m_\perp$, and this n dependence allows the event shape to directly probe hadron mass effects. In terms of Eq. (9) one trivially finds

$$f_{n,a}(r,y) = r^n e^{-|y|(1-a)} . \qquad (38)$$

These generalized angularities all have the same value of c_e,

$$c_{n,a} = \int_{-\infty}^{+\infty} dy\, e^{-|y|(1-a)} = \frac{2}{1-a} \equiv c_a , \qquad (39)$$

which from Table III is also the same as for classic angularities $\tau_{(a)}$. (Again $a < 1$ here.) Computing the function encoding the mass dependence we have

$$g_{n,a}(r) = \frac{(1-a)}{2} \int dy\, r^n e^{-|y|(1-a)} = r^n . \qquad (40)$$

Thus the $\tau_{(n,a)}$ event shapes belong to universality classes labeled by n, and represented by the functions

$$g_n(r) = r^n . \qquad (41)$$

Each value of n defines a different universality class, so in general there are infinitely many different event shape

c_e	τ	τ_2	$\tau_{(a)}$	C	$\rho_\pm$
Common	2	2	$\dfrac{2}{1-a}$	3π	1

TABLE III. Expression for the c_e coefficients for various dijet event shapes from Table II. Since c_e are defined using $f_e(1,y)$, they have the same value in each class.

$g_e(r)$	τ	τ_2	$\tau_{(a)}$	C	$\rho_\pm$
Original	$g_\tau(r)$	1	r	$\frac{2r^2}{\pi}K(1-r^2)$	1
P-scheme	$g_\tau(r)$	$g_\tau(r)$	$g_{\tau_a}(r)$	$\frac{2r^2}{\pi}K(1-r^2)$	$g_\tau(r)$
E-scheme	r	r	r	r	r
R-scheme	r	r	r	r	r
J-scheme	1	1	1	1	1

TABLE IV. The functions $g_e(r)$ of transverse velocity r for various dijet event shapes from Table II. Event shapes with the same $g(r)$ belong to the same universality class.

universality classes. For the r^n class, the universal power correction from Eq. (36) is

$$\Omega_1^n \equiv \int_0^1 \mathrm{d}r\, r^n\, \Omega_1(r). \qquad (42)$$

This procedure, of generalizing an event shape to obtain different sensitivity to hadron mass effects by multiplying by r^n, can just as easily be applied to event shapes other than angularities. By choosing large values of n, we preferentially select out particles whose transverse momentum is large compared to its mass. This might be useful in an experimental context to deweight the contribution of soft particles to event shapes, beyond the linear suppression in $m_\perp$ necessary for infrared safety.

We have included a summary of some common universality classes in Table V. For $n = 0$ and $n = 1$, the universality classes correspond with two that appear for classic event shapes, so we will also refer to $g(r) = 1$ as the Jet Mass class and $g(r) = r$ as the E-scheme class.

In Sec. V D, we will show that Pythia 8 and Herwig++ do indeed exhibit universality when holding n fixed but varying a, but as expected yield different power correction parameters Ω_1^n when n is varied.

C. Classic Event Shapes and Mass Schemes

In this subsection, we discuss c_e and $g_e(r)$ for the more traditional event shapes enumerated in Tab. I, and show how $g_e(r)$ changes when using various measurement schemes for hadron masses. Results for the corresponding $f_e(r,y)$ were summarized above in Table II. As already mentioned, the results for c_e are independent of the measurement scheme for hadron masses, and can be

computed directly with Eq. (35). For the various classic event shapes they are summarized in Table III.

For the event shapes in Tab. I with their original definitions, integrating their $f_e(r,y)$ over y we find

$$g_\tau(r) = 1 - E(1-r^2) + r^2\, K(1-r^2), \quad (43)$$
$$g_{\tau_2}(r) = g_{\rho_\pm}(r) = 1,$$
$$g_{\tau_{(a)}}(r) = r,$$
$$g_C(r) = \frac{2\, r^2}{\pi} K(1-r^2),$$

where E and K are the complete elliptic integrals

$$E(x) = \int_0^{\pi/2} \mathrm{d}\theta\, (1 - x\sin^2\theta)^{1/2}, \qquad (44)$$
$$K(x) = \int_0^{\pi/2} \mathrm{d}\theta\, (1 - x\sin^2\theta)^{-1/2}.$$

A plot of the $g(r)$'s in Eq. (43) is displayed in Fig. 2.

Direct analogs of $g_\tau(r)$, $g_C(r)$, $g_{\rho_\pm}(r)$ were computed in Ref. [1]. The translation from their notation (superscripts SW) to ours is $c_e^{\mathrm{SW}} = c_e$ and $\delta c_e^{\mathrm{SW}}(m^2/p_\perp^2) = c_e[\,g_e(r)/r - 1\,]$. Fig. 1 of Ref. [1] plots $(1 + \delta c_e^{\mathrm{SW}}/c_e^{\mathrm{SW}})$ versus $p_\perp/m$, which is the direct analog of our Fig. 2. In our figure, the function is bounded because of our use of the $r = p_\perp/m_\perp$ variable rather than $p_\perp/m$. These bounded $g(r)$ functions are more convenient for our basis discussion in Sec. IV D below.

By looking for event shapes with common $g(r)$'s in Eq. (43) or Fig. 2 we see that $\rho_\pm$ and τ_2 are in the "Jet Mass" universality class, and that the angularities $\tau_{(a)}$ for any a belong to a "E-scheme" universality class. Defining Ω_1^ρ and Ω_1^E as the universal power corrections for the Jet Mass and E-scheme classes, respectively, and accounting

Class	$g(r)$	Event shape
Jet Mass class (Ω_1^0 or Ω_1^ρ)	1	$\rho_\pm,\ \tau_2,\ \tau^J,\ \tau_{(a)}^J,\ C^J$
E-scheme class (Ω_1^1 or Ω_1^E)	r	$\tau_{(a)},\ \tau^E=\tau_2^E,\ C^E,\ \rho_\pm^E,\ \tau^R,\ \tau_{(a)}^R,\ C^R,\ \rho_\pm^R$
r^n class (Ω_1^n)	r^n	generalized angularities $\tau_{(n,a)}$ in Eq. (37)
Thrust class ($\Omega_1^{g_\tau}$)	$g_\tau(r)$	$\tau,\ \rho_\pm^P,\ \tau_2^P$
C-parameter class ($\Omega_1^{g_C}$)	$g_C(r)$	C
r^2 class (Ω_2^n)	r^2	$\tau_{(2,a)},\ \tau_{(a\to-\infty)}^P$

TABLE V. Event shape classes with a universal first power correction parameter $\Omega_1^{g_e}$. For a given event shape, the full power correction is $\Omega_1^e = c_e \Omega_1^{g_e}$.

for the c_e factors, we have

$$\Omega_1^{\tau_2} = 2\,\Omega_1^\rho, \qquad \Omega_1^{\tau_{(a)}} = \frac{2}{1-a}\,\Omega_1^E. \qquad (45)$$

Thrust and the C-parameter have their own $g(r)$ functions and hence among these event shapes are alone in their universality classes, with power corrections Ω_1^τ and Ω_1^C.[9]

We now consider the various hadron mass schemes. For all of the event shapes in Tab. I in the E-scheme, one has a common $g_e(r) = r$, so they all belong to the "E-scheme" universality class. It was for this reason that Ref. [1] considered the E-scheme to be privileged hadron mass scheme. In this sense, universality in the E-scheme is closest to the universality for massless particles, since any event shape that can written as a function of four-vectors has an E-scheme definition and they all have the same universal power correction. For event shapes defined directly in terms of $m_\perp$, r, and y (e.g. the generalized angularities in Eq. (37)), the E-scheme can be defined by first expressing the event shape in terms of four-vectors (with no explicit m dependence), and then applying the E-scheme replacement in Eq. (13). Then any E-scheme observable has $g(r) = r$ and hence is in the E-scheme class. An example of an exception are event shapes that vanish in the massless limit, $g_e(r = 1) = 0$, which do not have a meaningful E-scheme definition.

From Table IV, we see that the event shapes measured in the R-scheme also fall into the E-scheme class ($g(r) = r$), while event shapes measured in the J-scheme fall into the Jet Mass class ($g(r) = 1$). The fact that E-scheme and R-scheme jet shapes are in a common universality class is a non-trivial consequence of the relation $\partial\eta/\partial y = 1/v$ from Eq. (11).

For the P-scheme, universality classes are more complicated. Carrying out the integral in Eq. (35) to find

the $g(r)$'s one finds that thrust and the C-parameter are unchanged. For the jet masses and 2-jettiness $g_{\rho_\pm^P}(r) = g_{\tau_2^P}(r) = g_\tau(r)$, so both $\rho_\pm^P$ and τ_2^P belong to the thrust universality class:

$$\Omega_1^{\rho_\pm^P} = \frac{1}{2}\Omega_1^{\tau_2^P} = \frac{1}{2}\Omega_1^\tau \equiv \Omega_1^{g_\tau}. \qquad (46)$$

For P-scheme angularities, $g_{\tau_{(a)}^P}(r)$ does not appear to have a simple analytic formula for arbitrary a (although it is easy to compute numerically). By making a change of variables $y = -\ln\tan(\chi/2)$, a convenient way of writing it is

$$g_{\tau_{(a)}^P}(r) = (1-a)\int_0^{\pi/2}\mathrm{d}\chi\ \frac{\left(\sqrt{1-(1-r^2)\sin^2\chi}+\cos\chi\right)^{a-1}}{r^{a-2}\,\sin^a\chi}. \qquad (47)$$

For integer values, it is simple to find an analytic form, and for $a = -1, -2$ we find[10]

$$g_{\tau_{(-1)}^P}(r) = 2 - r - 2\left(\frac{1}{r}-r\right)\ln(1+r), \qquad (48)$$

$$g_{\tau_{(-2)}^P}(r) = 9 - \frac{8}{r^2} - \left(7-\frac{8}{r^2}\right)E(1-r^2) - (4-3\,r^2)\,K(1-r^2).$$

For any a, $g_{\tau_{(a)}^P}(0) = 0$ and $g_{\tau_{(a)}^P}(1) = 1$. For large negative values of a one finds

$$g_{\tau_{(a\to-\infty)}^P}(r) = r^2. \qquad (49)$$

Hence angularities in the P-scheme for large negative a belong to the same class as the generalized angularities in Eq. (37) for $n = 2$, with $\Omega_1^{\tau_{(a\to-\infty)}^P} = \Omega_1^{\tau_{(2,a)}}$.

In practice, $g_{\tau_{(a)}^P}(r)$ for arbitrary a quickly converges towards $g_{\tau_{(-\infty)}^P}(r)$, and hence there is a quasi-universality

---

[9] Accounting for the c_e dependence, the universal power corrections for the thrust and C-parameter classes are $\Omega_1^{g_\tau} = \Omega_1^\tau/2$ and $\Omega_1^{gC} = \Omega_1^C/3\pi$.

[10] In general for odd a, $g(r)$ involves only $\ln(1+r)$ and for even a only the elliptic functions $K(1-r^2)$ and $E(1-r^2)$ appear.
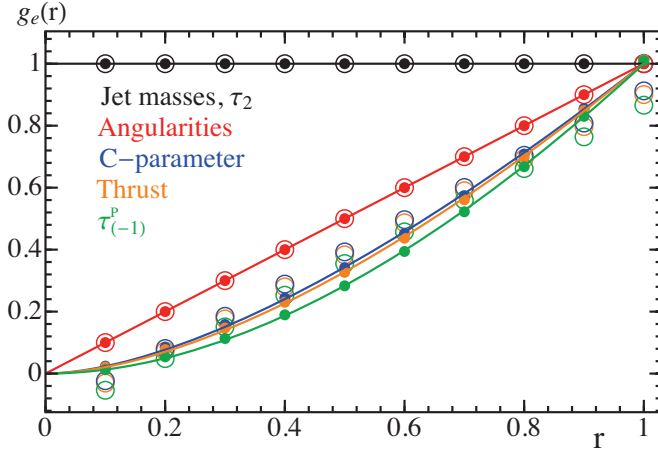
FIG. 2. From top to bottom the $g_e(r)$ functions for Jet Masses and 2-jettiness, Angularities, C-parameter, Thrust, and the P-scheme angularity with $a = -1$. Lines correspond to exact numerical values, open circles to two terms from the basis of Sec. IV D, and filled circles to three terms from the basis.

	b_0	b_1	b_2	b_3
Jet masses, τ_2	1	0	0	0
Angularities	$\dfrac{1}{2}$	$\dfrac{1}{2\sqrt{3}}$	0	0
Thrust	0.383	0.299	0.050	−0.006
$\tau_{(-1)}^P$	0.355	0.295	0.064	−0.004
C-parameter	0.393	0.300	0.046	−0.007
$\tau_{(a\to-\infty)}^P$	$\dfrac{1}{3}$	$\dfrac{1}{2\sqrt{3}}$	$\dfrac{1}{6\sqrt{5}}$	0

TABLE VI. Numerical value of the coefficients of the complete basis for the various $g_e(r)$ functions.

for angularities in the P-scheme. Also $g_C(r)$ and $g_\tau(r)$ are not so different from $g_{\tau_{(-\infty)}^P}(r)$, implying an approximate universality between event shapes in different classes for all event shapes in the P-scheme. This was already noted for thrust and the C-parameter in Ref. [1]. We will next develop a complete basis for describing $g_e(r)$ functions that will allow us to make this observation more quantitative.

D. Orthogonal Basis for $\Omega_1(r)$

Many $g_e(r)$ curves are still parametrically close, even if the corresponding event shapes are formally in different universality classes. Examples are thrust, C-parameter, and $\tau_{(-1)}^P$ angularity shown in Fig. 2. To get a quantitative handle on this observation, we can use a complete set of orthonormal functions for $r \in [0,1]$:

$$h_n(r) \equiv \sqrt{2n+1}\, P_n(2r-1)\,, \qquad (50)$$

$$\int_0^1 dr\, h_n(r)\, h_m(r) = \delta_{nm}\,,$$

where P_n are the Legendre polynomials. Now we can decompose any of the $g_e(r)$ functions in this basis in the usual way:

$$g_e(r) = \sum_{n=0}^\infty b_n^e\, h_n(r)\,, \qquad (51)$$

$$b_n^e = \int_0^1 dr\, g_e(r)\, h_n(r)\,.$$

Since the $g(r)$ functions for classic event shapes are fairly close to low-order polynomials, the first few terms in the basis will provide an accurate approximation.

The values of the b_n^e coefficients are shown in Table VI for the classic event shapes. The approximation for the $g_e(r)$ functions are plotted in Fig. 2, where the exact values are shown by lines and the approximation with two terms from the basis (b_0, b_1) are shown by hollow circles, and with three terms (b_0, b_1, b_2) by filled circles. For the jet masses, 2-jettiness, and angularities, the approximate result is exact with two terms in the basis. For the remaining events shapes, the approximation with two terms is likely sufficiently accurate at the level one expects of current experimental and perturbative precision. With three terms, the approximation is excellent in all cases, so the third term can be regarded as a high-precision correction. This is also apparent from the values in Table VI, where b_0 and b_1 are much larger than b_2 (and computing $b_{n>2}$ one finds they are negligible).

Using Eq. (50) one can write any Ω_1^e in terms of a denumerable set of power correction parameters:

$$\Omega_1^e = \sum_{n=0}^\infty b_n^e\, \Omega_1^{(n)}\,, \qquad \Omega_1^{(n)} = \int_0^1 dr\, h_n(r)\, \Omega_1(r)\,. \quad (52)$$

Only the first few terms will be numerically relevant for most event shape observables. Using Eqs. (51) and (52) and the results in Table VI, we can make the following exact identifications

$$\Omega_1^{(0)} = \Omega_1^\rho\,, \qquad \Omega_1^{(1)} = 2\sqrt{3}\,\Omega_1^E - \sqrt{3}\,\Omega_1^\rho\,. \qquad (53)$$

Thus the power correction parameters for the Jet Mass class and E-Scheme class already give an excellent approximation for the various classic event shapes. To refine the prediction even further one can use the next term in the basis, $\Omega_1^{(2)}$.[11] Writing the leading power correction for the other event shapes in terms of Ω_1^ρ, Ω_1^E, and $\Omega_1^{(2)}$ we have:

$$\Omega_1^\tau = 1.034\,\Omega_1^E - 0.135\,\Omega_1^\rho + 0.050\,\Omega_1^{(2)}\,, \qquad (54)$$

---

[11] In principle, we could extract $\Omega_1^{(2)}$ exactly from the $\tau_{(a\to-\infty)}^P$ power correction, since from Table VI, we see that $g_{\tau_{(a\to-\infty)}^P}(r)$ is saturated by the first three terms in the Legendre expansion.

$$\Omega_1^C = 1.039\,\Omega_1^E - 0.127\,\Omega_1^\rho + 0.046\,\Omega_1^{(2)}\,,$$
$$\Omega_1^{\tau_{(-1)}^P} = 1.022\,\Omega_1^E - 0.156\,\Omega_1^\rho + 0.064\,\Omega_1^{(2)}\,.$$

In general both the Ω_1^E and Ω_1^ρ terms are numerically important since experiment favors values $\Omega_1^E \sim \Omega_1^\rho/2$, and $\Omega_1^{(2)}$ can be typically neglected. However, since the numerical coefficients in Eq. (54) are so close, one is justified in using the approximation $\Omega_1^\tau \simeq \Omega_1^C \simeq \Omega_1^{\tau_{-1}^P}$ up to corrections of $\sim 15\%$.

We note that the above basis analysis is valid only at a fixed value of Q since $\Omega_1(r,\mu)$ has an anomalous dimension which we will compute in Sec. V, and the appropriate μ scales with Q. As we will see in Sec. V C, we will need to refine the above analysis in order to relate power corrections at different values of Q.

E. Renormalon-free Definition of $\Omega_1(r)$

It is well known that the first moment of a perturbative event shape distribution has a $\Lambda_{\rm QCD}$ renormalon ambiguity in the $\overline{\rm MS}$ scheme [77], which corresponds to a renormalon in the $\overline{\rm MS}$ power correction parameter Ω_1^e that we have been considering so far. To our knowledge, the only renormalon-based analysis of event shapes that observes sensitivity to hadron masses is Ref. [39] (which in turn, called into question the massless universality results). In this section we argue that the universality relations given in Sec. IV A will remain unchanged as long as one defines appropriate renormalon-free schemes for the $1/Q$ power corrections.

In general the $\Lambda_{\rm QCD}$ renormalon is removed by converting the power correction parameter to a new scheme

$$\Omega_1^e(R,\mu) \equiv \Omega_1^e(\mu) - \delta_e(R,\mu)\,, \qquad (55)$$

where $\delta_e(R,\mu)$ is a series in $\alpha_s(\mu)$. There is a corresponding change to the perturbative part of the cross section that depends on this same series. Writing $\hat{\sigma}_e(x)$ for the Fourier transform of $d\hat{\sigma}/de$ this change is

$$\hat{\sigma}_e(x) \to \tilde{\sigma}_e(x) = \hat{\sigma}_e(x)\,e^{-ix\,\delta_e(R,\mu)/Q}\,. \qquad (56)$$

Recall that universality classes relate $\Omega_1^e(\mu)$ for different event shapes e, and that the relations are nonperturbative. Hence it is clear that one has the *same* renormalon ambiguity for event shapes that are members of the same class (differing only by the proportionality constants c_e). Thus it is sufficient to adopt a common scheme change for members of the same class via any scheme satisfying

$$\delta_e(R,\mu) = c_e\,R\,e^{\gamma_E} \sum_{n=1}^\infty \left(\frac{\alpha_s(\mu)}{4\pi}\right)^n \delta_n^{(g_{e'})}(\mu/R)\,. \qquad (57)$$

Here the $\delta_n^{(g_{e'})}(\mu/R)$ coefficients involve factors of $\ln(\mu/R)$ and are chosen such that the new $\Omega_1^e(R,\mu)$ is

free of the leading $\Lambda_{\rm QCD}$ renormalon ambiguity. The numerical values for $\delta_n^{(g_{e'})}$ will depend on the representative e' that we choose, but any representative has the same renormalon and hence is a valid subtraction series for all members of the g_e class.

One popular scheme for fixing the coefficients $\delta_n^{(g_{e'})}(\mu/R)$ is based on the dispersive approach, where $R = \mu_I$ [36–38]. In this framework to obtain an appropriate subtraction at $\mathcal{O}(\alpha_s^2)$ one must also include the Milan factor [38, 45]. As as typical of scheme changes based on QCD perturbation theory, this scheme removes the renormalon for the massless limit $r = 1$.

At higher orders in α_s a more convenient scheme uses the leading power perturbative soft function itself [62], $S_e^{\rm pert}$, which does not require additional computations beyond those needed for a resummed analysis of the event shape. Again this scheme change removes the renormalon for the massless limit $r = 1$. For each g_e universality class we pick a representative e' that is a member of the class. Then for all event shapes $e \in g_e$ we define[12]

$$\delta_e(R,\mu) = \frac{c_e}{c_{e'}}\,R\,e^{\gamma_E}\,\frac{d}{d\ln(ix)} \ln S_{e'}^{\rm pert}(x,\mu)\bigg|_{x=(iRe^{\gamma_E})^{-1}}\,. \qquad (58)$$

For $e = \tau$ Eq. (58) yields the subtractions for thrust defined in Ref. [78]. Given that renormalons probe the infrared structure of amplitudes, one might naively expect that different subtractions would be necessary for the different universality classes, since they treat hadron masses differently. However, the scheme change in Eq. (58) is based solely on the QCD perturbative calculation of $S_{e'}^{\rm pert}$ with $r = 1$, so only the c_e coefficients will differ in subtractions for different event shapes. Thus in this setup, the same subtraction $\delta_{e'}(R,\mu)$ can be chosen for all universality classes.
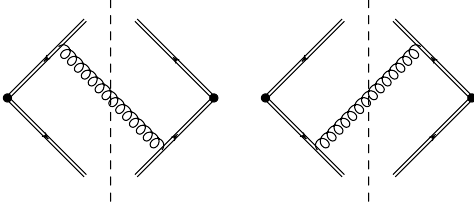
In App. B we carry out a standard renormalon bubble sum calculation for an arbitrary dijet event shape e satisfying Eq. (9) and demonstrate that Eq. (58) yields a perturbative cross section $\tilde{\sigma}_e(x)$ and power correction parameter $\Omega_1(R,\mu)$ that are free from the $\Lambda_{\rm QCD}$ renormalon probed by this method. It might be interesting to consider extensions of Eq. (58) that satisfy Eq. (57) but have additional dependence on hadron mass effects.

V. ANOMALOUS DIMENSION OF $\Omega_1(r)$

A. Running at One-Loop

In this section, we compute the one-loop anomalous dimension of the QCD matrix element $\Omega_1(r,\mu)$ in the

---

[12] To facilitate a multiplicative renormalization structure and to account for non-Abelian exponentiation, one uses the logarithmic derivative of the position space soft function $S_e^{\rm pert}(x,\mu)$ [78], a definition adapted from the top jet-mass definition of Ref. [79].

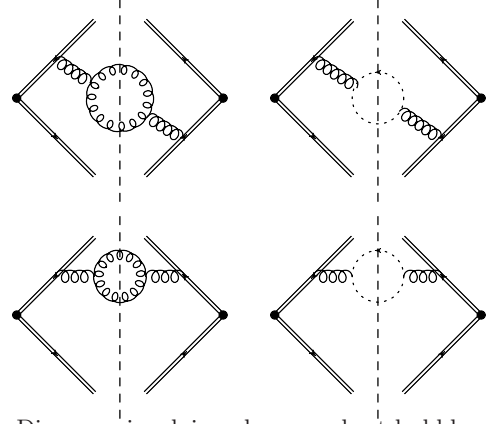FIG. 3. Tree level graphs for $\Omega_1(r, \mu)$.

FIG. 4. Diagrams involving gluon or ghost bubbles with two cut particles. The 4 additional diagrams obtained by a flip about the horizontal or vertical axis are not shown. Diagrams with one cut particle for wavefunction renormalization and coupling renormalization are also not displayed.

FIG. 5. Purely Abelian $\mathcal{O}(\alpha_s^2)$ diagrams. Either gluon line crossing the cut can be the source. The 4 additional diagrams obtained by a flip about the horizontal or vertical axis are not shown.

$\overline{\text{MS}}$ scheme, with details given in App. C. We regulate the UV with dimensional regularization (DR) using $d = 4 - 2\epsilon$.

Since $\Omega_1(r)$ has mass-dimension one and is proportional to the infrared (IR) scale Λ_{QCD}, one must be careful to establish IR regulators for the perturbative calculation in such a way that there is nonzero overlap with the operator matrix element. This requires at least one dimensionful IR regulator, as well as a mechanism to probe different values of r. With this, we can then compute the anomalous dimension just as we would for any external operator in QCD. The anomalous dimension will be independent of the precise IR procedure used to identify the matrix element.

A convenient choice for the IR regulator is obtained by coupling a massive adjoint background source $J^{\mu A}$ to the Wilson lines in $\Omega_1(r)$ by the replacement

$$A^{\mu A}(x) \to A^{\mu A}(x) + J^{\mu A}(x) \qquad (59)$$

in Eq. (18) and in the QCD Lagrangian. There is no Lagrangian mass term for the source $J^{\mu A}$, but for it to serve as an IR regulator, we will consider it to carry a massive particle momentum q^μ where $q^2 = m^2$. Recall from Eq. (25) that the $\mathcal{E}_T(r, 0)$ operator in $\Omega_1(r)$ sums over contributions from individual particles in the final state. If $\mathcal{E}_T(r, 0)$ acts on any particle other than $J^{\mu A}$, then the corresponding phase space integral is scaleless and dimensionful, and hence vanishes in DR. Thus the first nonzero contribution occurs where $\mathcal{E}_T(r, 0)$ acts on a $J^{\mu A}$ (and we then set all other $J^{\mu A}$'s to zero). This IR regulator is convenient for bookkeeping and does not overly complicate the evaluation of loop integrals. Effectively it amounts to considering one of the final state gluons, namely the one acted upon by $\mathcal{E}_T(r, 0)$, as having mass m and thus $r \neq 1$. For convenience when drawing Feynman diagrams, we use the same notation for massless gluons and the source, and simply note that we must sum over the cases where each final state gluon is the source.

At tree level, as shown in Fig. 3, we have only the source line. This yields the nonzero matrix element

$$M_1^{\text{tree}}(r) = \frac{2\alpha_s C_F}{\pi} \frac{m\,r}{(1 - r^2)^{\frac{3}{2}}} \,. \qquad (60)$$

Hence our setup provides nonzero overlap with the operator in $\Omega_1(r)$.
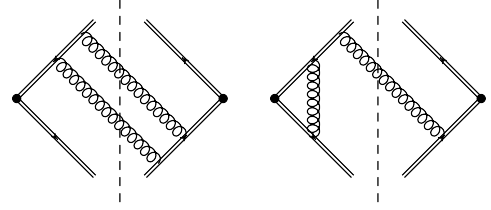
We now turn our attention to the $\mathcal{O}(\alpha_s^2)$ corrections. Here we must fix a gauge for the $A^{\mu A}$ massless gluons. We have carried out all our calculations both with traditional Feynman gauge, as well as with a background field Feynman gauge where the source $J^{\mu A}$ takes the place of the external background field. Both yield the same results. In addition to $J^{\mu A}$, we must introduce extra IR regulators specific to individual diagrams. We find that shifting eikonal propagators involving the loop or phase-space momentum k^μ by $n \cdot k \to n \cdot k + \Delta_n$ and $\bar{n} \cdot k \to \bar{n} \cdot k + \Delta_{\bar{n}}$ suffices to regulate other IR divergences.

For the diagrams in Fig. 4 which involve two particles in the final state through either a ghost bubble, or a gluon bubble, the sum of graphs does not involve a UV divergence (moreover these graphs are IR finite). Hence they can be ignored for the purposes of calculating the anomalous dimension. The remaining diagrams are either Abelian with color factor C_F^2 or non-Abelian with color factor $C_F C_A$. Abelian contributions are shown in Figs. 5 and 6, and in the sum over Abelian diagrams, the real radiation and virtual contributions exactly cancel (for all ϵ). It is easy to prove that this cancellation happens to all orders in perturbation theory. This proof uses the fact that $Y[A + J] = Y[A]Y[J]$ for an Abelian theory with no light quarks, and that $Y[A]Y^\dagger[A] = 1$.
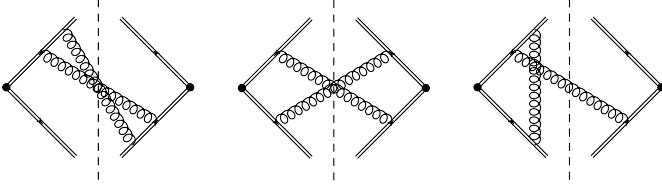
FIG. 6. Independent emission diagrams with Abelian and non-Abelian contributions. The 4 additional diagrams obtained by a horizontal flip or complex conjugation are not shown.

This leaves just the non-Abelian diagrams coming from Fig. 6, and triple gluon vertex diagrams in Fig. 7. There is also a contribution from gauge coupling renormalization which is not just canceled by the vacuum polarization graphs in many gauges. For the $1/\epsilon$ poles, we can take $\Delta_{n,\bar{n}} \to 0$ in the sum of graphs in Fig. 6 and seperately in Fig. 7, so the extra IR regulators cancel out of the UV terms as expected. The sum of diagrams in Fig. 6 and the sum in Fig. 7 each have $1/\epsilon^2$ poles, but these cancel in the complete sum. This leaves only a nonzero $1/\epsilon$ pole which will yield the anomalous dimension.

The final result for the UV divergence in the matrix element of the bare $\Omega_1(r)$ operator is

$$M_1^{\text{1-loop}}(r) = \left(- \frac{\alpha_s C_A}{2\pi\epsilon} \ln(1 - r^2) \right) M_1^{\text{tree}}(r). \quad (61)$$

We define the renormalized $\overline{\text{MS}}$ operator by

$$\Omega_1^{\text{bare}}(r) = Z(r, \mu, \epsilon) \, \Omega_1(r, \mu), \quad (62)$$

so Eq. (61) determines $Z(r, \mu, \epsilon)$ at $\mathcal{O}(\alpha_s)$. Using $\mu \, d\alpha_s/d\mu = -2\epsilon\,\alpha_s + \dots$, the one-loop anomalous dimension of $\Omega_1(r)$ is

$$\mu \frac{d}{d\mu} \Omega_1(r, \mu) = \left[- \frac{\alpha_s C_A}{\pi} \ln(1 - r^2) \right] \Omega_1(r, \mu). \quad (63)$$

Note that this anomalous dimension is positive since $\ln(1 - r^2) < 0$.

Intriguingly, the anomalous dimension is r-dependent, showing the important role of hadron masses. However, there is no mixing for operators at different values of r, so this RGE can be solved exactly to yield

$$\Omega_1(r, \mu) = \Omega_1(r, \mu_0) \left[\frac{\alpha_s(\mu)}{\alpha_s(\mu_0)} \right]^{\frac{2\,C_A}{\beta_0} \ln(1 - r^2)} \quad (64)$$

$$= \Omega_1(r, \mu_0) \left[1 - r^2 \right]^{\frac{2\,C_A}{\beta_0} \ln \frac{\alpha_s(\mu)}{\alpha_s(\mu_0)}}.$$

Here one can consider $\mu_0 \sim 2$ GeV as the low energy hadronic scale where we specify the nonperturbative matrix element, and μ as a high energy scale that is appropriate for the observable being considered. In Sec. V B we will show that $\mu \simeq Qe$ for the region of event shape distributions with $e \ll e_{\max}$ and $Qe \gg \Lambda_{\text{QCD}}$, and $\mu \simeq Qe_{\max}$ for first moments of event shapes.
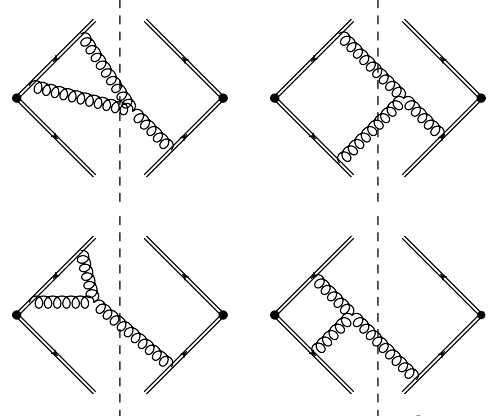

FIG. 7. Triple gluon Y-diagrams for the $\mathcal{O}(\alpha_s^2)$ correction to $\Omega_1(r)$. The 12 additional diagrams obtained by a horizontal flip or complex conjugation are not shown. Diagrams with all 3 gluons coupled to Wilson lines of the same direction vanish.

In order to use the resummed expression for $\Omega_1(r, \mu)$ to predict the evolution from $\Omega_1^e(\mu_0)$ to $\Omega_1^e(\mu)$, one would need to know the full r-dependence of $\Omega_1(r, \mu_0)$ to perform the integral over $g_e(r)$. We will see how to approximately circumvent this problem in Sec. V C.

One can also consider expanding Eq. (64) perturbatively in $\alpha_s(\mu_0)$ which yields

$$\Omega_1(r, \mu) = \Omega_1(r, \mu_0) \quad (65)$$

$$\times \left[1 - \frac{\alpha_s(\mu_0) C_A}{\pi} \ln \left(\frac{\mu}{\mu_0} \right) \ln(1 - r^2) + \dots \right].$$

If one truncates at $\mathcal{O}(\alpha_s)$, then one only needs two nonperturbative parameters defined at μ_0 to determine the the power corrections for an event shape at a higher scale μ:

$$\Omega_1^e(\mu) = \Omega_1^e(\mu_0) + \frac{\alpha_s(\mu_0) C_A}{\pi} \ln \left(\frac{\mu}{\mu_0} \right) \Omega_1^{e,\,\ln}(\mu_0). \quad (66)$$

Here $\Omega_1^e(\mu_0)$ is our standard power correction parameter at the scale μ_0 given by Eq. (36) with $\Omega_1(r, \mu_0)$, and the slope parameter $\Omega_1^{e,\,\ln}(\mu_0)$ is defined by

$$\Omega_1^{e,\,\ln}(\mu_0) \equiv - \int dr \, \ln(1 - r^2) \, c_e \, g_e(r) \, \Omega_1(r, \mu_0). \quad (67)$$

The expanded form in Eq. (66) is a reasonable approximation if μ is not too different from μ_0. It works for a larger range than one would naively expect since there are numerical cancellations in the $\mathcal{O}(\alpha_s^2)$ term between $\ln^2(1 - r)$ and $\ln(1 - r)$ contributions.

B. The Wilson Coefficient of $\Omega_1(r, \mu)$

Having established that the nonperturbative matrix element $\Omega_1(r, \mu_0)$ runs, we reconsider the operator expansion of the shape function $F_e(\ell)$ in Eq. (16), now incorporating α_s corrections through a Wilson coefficient

$C_1^e(\ell, r, \mu)$ for $\Omega_1(r, \mu)$. The formula in Eq. (16) becomes

$$
F_e(\ell) = \delta(\ell) + \int dr\, C_1^e(\ell, r, \mu)\, c_e\, g_e(r)\, \Omega_1(r, \mu)
$$
$$
+ \mathcal{O}\Big(\frac{\Lambda_{\rm QCD}^2}{\ell^3}\Big). \tag{68}
$$

As usual the μ dependence of $C_1^e(\ell, r, \mu)$ cancels that of $\Omega_1(r, \mu)$. The dependence of $C_1^e(\ell, r, \mu)$ on ℓ and μ will determine the appropriate scale μ where there are no large logarithms in this Wilson coefficient. This in turn will determine the appropriate perturbative scale μ for the endpoint of the evolution derived in Eq. (64). Since the ℓ dependence is treated differently by event shape distributions and by their first moments, a different scale μ will be found for these two observables.

Taking Eq. (63) together with the cancellation of the μ dependence implies

$$
\mu \frac{d}{d\mu} C_1^e(\ell, r, \mu) = \frac{C_A \alpha_s(\mu)}{\pi} \ln(1 - r^2) C_1^e(\ell, r, \mu). \tag{69}
$$

At order α_s using Eq. (16) this becomes

$$
\mu \frac{d}{d\mu} C_1^e(\ell, r, \mu) = -\frac{C_A \alpha_s(\mu)}{\pi} \ln(1 - r^2)\, \delta'(\ell). \tag{70}
$$

Note that $C_1^e(\ell, r, \mu)$ must have mass dimension -2. At $\mathcal{O}(\alpha_s)$ the simplest potential solution has the dependence $\ln(\mu/\kappa)\delta'(\ell)$, but by dimensional analysis the only possibility for κ is ℓ which leads to a singular result. The correct solution is

$$
C_1^e(\ell, r, \mu) = -\delta'(\ell) + \frac{C_A \alpha_s(\mu)}{\pi} \ln(1 - r^2) \frac{d}{d\ell}\left(\frac{1}{\mu}\Big[\frac{\mu}{\ell}\Big]_+\right)
$$
$$
+ \frac{\alpha_s(\mu)}{\pi} \delta'(\ell)\, d_1^e(r) + \mathcal{O}(\alpha_s^2), \tag{71}
$$

which can be deduced since the derivative of the plus function has the right dimension and has the required logarithmic scale dependence

$$
\mu \frac{d}{d\mu} \frac{d}{d\ell} \frac{1}{\mu}\Big[\frac{\mu}{\ell}\Big]_+ = -\delta'(\ell). \tag{72}
$$

In this way, the plus function term in the Wilson coefficient exactly compensates for the first order $\alpha_s(\mu)\ln(\mu)$ dependence in $\Omega_1(r, \mu)$. Note that

$$
\frac{d}{d\ell} \frac{1}{\mu}\Big[\frac{\mu}{\ell}\Big]_+ = -\frac{1}{\mu^2}\Big[\frac{\mu^2}{\ell^2}\Big]_{++} + \frac{1}{\mu}\delta(\ell), \tag{73}
$$

where the $++$-distribution induces two subtractions about $\ell = 0$ and is defined so that its zeroth and first moments integrate to zero for the limits $\ell/\mu \in [0, 1]$.

The function $d_1^e(r)$ in Eq. (71) is also a perturbatively computable contribution to the Wilson coefficient. The matching calculation for this term involves considering the difference between renormalized Feynman diagrams for the full theory soft function matrix element

$$
S_e(\ell) = \langle 0| \overline{Y}_{\bar n}^\dagger Y_n^\dagger \delta(\ell - Q\hat e) Y_n \overline{Y}_{\bar n} |0\rangle \tag{74}
$$

and for the low-energy matrix elements describing $\Omega_1(r, \mu)$. A complete one-loop calculation of $d_1^e(r)$ is beyond the scope of our work. In App. D we carry out this matching procedure for thrust in order to directly derive the term that involves the derivative of the plus-function shown in Eq. (71). Many of the complications required to derive $d_1^e(r)$ do not enter for this term.

Next consider the impact of $C_1^e(\ell, r, \mu)$ on the distribution and first moment event shape observables discussed in Sec. II C, in order to determine the appropriate scale μ where large logs are minimized. For the differential distribution we find

$$
\frac{d\sigma}{de} = \frac{d\hat\sigma}{de} + \frac{1}{Q}\int d\ell \int dr \frac{d\hat\sigma}{de}\Big(e - \frac{\ell}{Q}\Big) C_1^e(\ell, r, \mu)
$$
$$
\times c_e\, g_e(r)\, \Omega_1(r, \mu)
$$
$$
= \frac{d\hat\sigma}{de} - \frac{1}{Q}\Big(\Omega_1^e(\mu) + \frac{\alpha_s(\mu)}{\pi}\Omega_1^{e,\,d}(\mu)\Big)\frac{d^2\hat\sigma}{de^2}(e)
$$
$$
+ \frac{\Omega_1^{e,\,\ln}(\mu)}{Q}\frac{\alpha_s(\mu)C_A}{\pi}\Bigg\{\ln\Big(\frac{\mu}{eQ}\Big)\frac{d^2\hat\sigma}{de^2}(e)
$$
$$
- \int_0^{eQ}\frac{d\ell}{\ell}\Big[\frac{d^2\hat\sigma}{de^2}\Big(e - \frac{\ell}{Q}\Big) - \frac{d^2\hat\sigma}{de^2}(e)\Big]\Bigg\}, \tag{75}
$$

where the nonperturbative parameter $\Omega_1^{e,\,\ln}(\mu)$ is given in Eq. (67), and

$$
\Omega_1^{e,\,d_1}(\mu) = \int dr\, d_1^e(r)\, c_e\, g_e(r)\, \Omega_1(r, \mu). \tag{76}
$$

The explicit $\ln(\mu/Qe)$ in Eq. (75) implies that for the distribution, the appropriate scale to run the power correction to is $\mu = Qe$.

For the first moment we find

$$
\langle e\rangle = \int_0^{e_{\max}} de\, e \int d\ell\, \frac{1}{\hat\sigma}\frac{d\hat\sigma}{de}\Big(e - \frac{\ell}{Q}\Big) F_e(\ell) \tag{77}
$$
$$
= \int de \int d\ell\, \theta\Big(e_m - e - \frac{\ell}{Q}\Big)\Big(e + \frac{\ell}{Q}\Big)\frac{1}{\hat\sigma}\frac{d\hat\sigma}{de}(e)\, F_e(\ell)
$$
$$
= \langle e\rangle_{\rm pert} + \frac{\Omega_1^e(\mu)}{Q} + \frac{\alpha_s(\mu)}{\pi}\frac{\Omega_1^{e,\,d}}{Q} + \frac{\Omega_1^{e,\,\ln}(\mu)}{Q}\frac{C_A\alpha_s(\mu)}{\pi}
$$
$$
\times \int_0^{e_{\max}}\frac{1}{\hat\sigma}\frac{d\hat\sigma}{de}(e)\Big[\ln\Big(\frac{\mu}{Q(e_{\max} - e)}\Big) - \frac{e^2}{e_{\max}(e_{\max} - e)}\Big]
$$

where the notation $\langle e\rangle_{\rm pert}$ is defined in Eq. (20). Since the perturbative moments generate a rapidly convergent series, we can expand the perturbative coefficient of $\Omega_1^{e,\,\ln}(\mu)$ in (e/e_m) to obtain

$$
\int_0^{e_{\max}} de\, \frac{1}{\hat\sigma}\frac{d\hat\sigma}{de}(e)\Big[\ln\Big(\frac{\mu}{Q(e_{\max} - e)}\Big) - \frac{e^2}{e_{\max}(e_{\max} - e)}\Big]
$$
$$
= \ln\Big(\frac{\mu}{Q e_{\max}}\Big) + \frac{\langle e\rangle_{\rm pert}}{e_{\max}} - \frac{\langle e^2\rangle_{\rm pert}}{2e_{\max}^2} + \cdots. \tag{78}
$$

Thus for the first moment the appropriate scale to run the power correction to is $\mu = Qe_{\max}$.

C. Orthogonal Basis for $\Omega_1(r, \mu)$

In Sec. IV D, we showed that the power corrections for observables in different universality classes could be approximately related by expanding out $g_e(r)$ and $\Omega_1(r, \mu)$ in a suitable basis. Since the appropriate scale μ for Ω_1 is Q dependent, this is true if all measurements are performed at a single Q. From Secs. V A and V B, we know that the leading power correction has nontrivial Q dependence, and we would like to incorporate this information in our description of $\Omega_1(r)$.

Immediately from Eq. (64), we see that $\Omega_1(r, \mu)$ will diverge as $r \to 1$. Even if $\Omega_1(r, \mu_0)$ is regular at some scale μ_0, it will quickly develop a singularity at $r = 1$ as μ evolves. This singularity can be physically interpreted as the propensity of Wilson lines to emit soft massless particles. Of course, this singularity is still square-integrable, and thus the power correction is still well-defined.[13] However the singularity at $r = 1$ means that if the Legendre polynomial basis in Sec. IV D is used at a scale μ_0 to define a basis for power corrections $\Omega_1^{(n)}(\mu_0)$, then it converges very slowly when trying to use these same parameters to describe power corrections for scales $\mu \gg \mu_0$ or $\mu \ll \mu_0$.

Looking at the α_s expansion of the running formula in Eq. (66), we see that to describe the power correction for a range of Q values, we must find a suitable basis to describe not only $g_e(r)$ and $\Omega_1(r, \mu_0)$ but also $g_e(r) \ln(1-r^2)$. Since $\ln(1 - r^2)$ is unbounded at $r = 1$ (but still square integrable), we will use the freedom to introduce additional square-integrable basis elements $(1 - r)^{-k}$ for suitable values $0 < k < 1/2$. As long as we are content to work with a finite number of basis elements, we can always make such a basis orthonormal via the Gram-Schmidt procedure. Adding these additional functional forms will in general yield an over-complete basis, but this is not an issue in practice since we will only ever consider a finite number of basis elements.

The situation becomes a bit more complicated if we consider the full running in Eq. (64). In general, any finite basis we choose to describe $\Omega_1(r, \mu)$ at one value of Q will not provide a good description at a different value of Q due to the running. In particular, a basis that is orthonormal at one value of μ_0 will no longer be orthonormal at another scale. Instead of trying to find a basis that works for any Q, we instead choose a scale μ_0 at which we model $\Omega_1(r, \mu_0)$, and then evolve according to Eq. (64). We then fit for the basis coefficients by using information at different values of Q. This procedure is philosophically the same as the procedure used to determine parton distribution functions (PDFs), where the PDFs are modeled at a low scale and then evolved to higher Q values via the DGLAP equations [80–82].

D. Comparison to Monte Carlo

We now show that power correction universality and running is exhibited by two widely used Monte Carlo programs: Pythia 8.162 [83] and Herwig++ 2.6.0 [84]. The hadronization model in Pythia 8 is based on string fragmentation while Herwig++ is based on cluster fragmentation.[14] The default hadronization parameters in both programs have been tuned to reproduce LEP e^+e^- event shapes at the Z pole. We will consider $e^+e^- \to$ hadrons at various Q values, turning off initial-state electromagnetic radiation to avoid the radiative return process.

Our study will use the generalized angularities $\tau_{(n,a)}$ defined in Eq. (37). Via the arguments in Sec. IV B, we know that the power corrections for different values of a are related via the $c_a = 2/(1-a)$ coefficients in Eq. (39),

$$\Omega_1^{\tau_{(n,a)}}(\mu) = c_a \, \Omega_1^n(\mu), \qquad (79)$$

where $\Omega_1^n(\mu)$ is the universal power correction for the r^n class given in Eq. (42).

From Eq. (21), we know that the leading power correction shifts the moments of event shapes, so we can extract the universal power corrections for the generalized angularities via the first moment

$$\Omega_1^n(\mu_Q) = \frac{1}{c_a} \left(Q \left\langle \tau_{(n,a)} \right\rangle - Q \left\langle \tau_{(n,a)} \right\rangle_{\text{pert}} \right), \qquad (80)$$

up to small higher-order corrections. Since the maximum value of thrust ($a = 0$) is $1/2$, we take $\mu_Q = Q/2$ to avoid having large logs in these higher order corrections, which were displayed above in Eq. (78).[15] The perturbative moment $\left\langle \tau_{(n,a)} \right\rangle_{\text{pert}}$ is the same for event shapes with a common $r \to 1$ limit. To form a combination that is sensitive to the power corrections in the Monte Carlo programs without having to know about their perturbative contributions, we consider the difference $\tau_{(0,a)} - \tau_{(n,a)}$ which compares the same value of a at two different values of n. For this combination we have

$$\Omega_1^0(\mu_Q) - \Omega_1^n(\mu_Q) = \frac{Q}{c_a} \left(\left\langle \tau_{(0,a)} \right\rangle - \left\langle \tau_{(n,a)} \right\rangle \right). \qquad (81)$$

Note that this difference is also independent of the additive scheme change that removes the renormalon from $\Omega_1^e(\mu)$, given by Eq. (55) with Eq. (58). Therefore we emphasize that our analysis in this section only probes the running in Eq. (63) and not the R-evolution [64, 65] associated with $\Omega_1^e(R, \mu)$.

---

[13] For evolution over a large enough Q range, the singularity may no longer be integrable, and may turn into a distribution, but we do not encounter this subtlety in our analysis.

[14] The two programs also have different showering models, with Pythia 8 using a $p_\perp$-ordered shower and Herwig++ using an angular-ordered shower. Since the showers are evolved down to the non-perturbative scale, part of the renormalization group evolution of the power correction may be captured by the showering algorithm, and not just the hadronization model.

[15] The angularities with $a \neq 1$ have different values for $e_{\max}$, but this is an $\mathcal{O}(1)$ change to the μ scale, and hence not relevant.
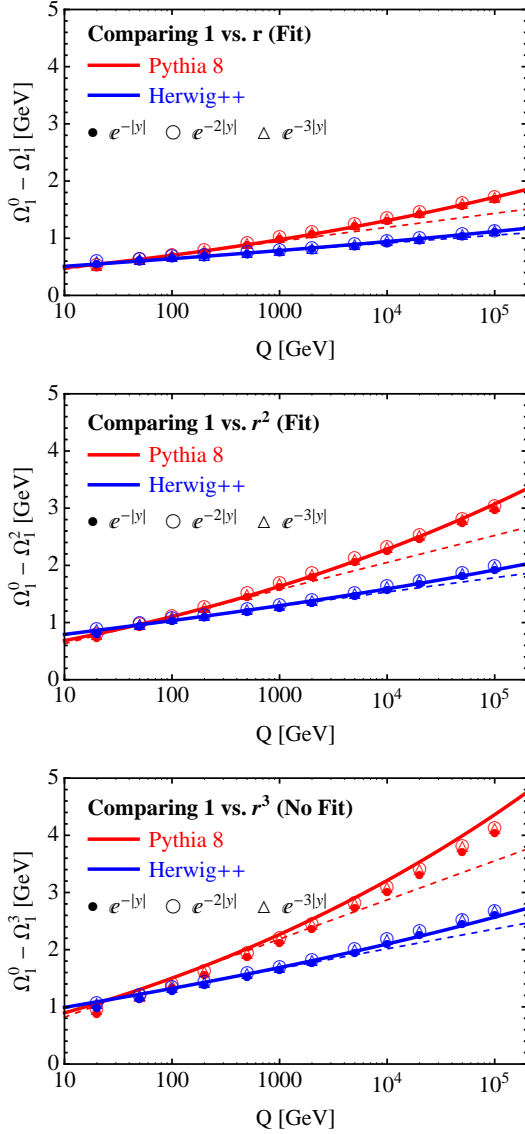
FIG. 8. Universal power corrections extracted from Pythia 8.162 and Herwig++ 2.6.0 for the generalized angularities $\tau_{(n,a)}$. We use the measured power corrections in the first two plots to fit for $\Omega(r,\mu_0)$ at $Q = 100$ GeV, using Eq. (64) to evolve to different Q scales. The curves in third plot are then predicted. The dashed curves show the approximate formula in Eq. (66).

In Fig. 8 we plot $\Omega_1^0 - \Omega_1^n$ for $a = 0, -1, -2$, $n = 1, 2, 3$, and Q values ranging from 20 GeV to 200 TeV. At a fixed scale Q, the power corrections are independent of a with at most 5% variations, thus demonstrating the anticipated universality.[16] Note that both programs were tuned to LEP Z pole and low energy data, so it is not surprising that they have the same power corrections at

---

[16] The leading violation of universality can be attributed to different matching coefficients $d_1^e(r)$ in Eq. (71).

	$Q = 100$ GeV		$Q = 10^4$ GeV	
	Pythia 8	Herwig++	Pythia 8	Herwig++
$\Omega_1^0 - \Omega_1^1$	0.7 GeV	0.6 GeV	1.3 GeV	0.9 GeV
$\Omega_1^{0,\,\ln} - \Omega_1^{1,\,\ln}$	0.9 GeV	0.5 GeV	2.4 GeV	1.1 GeV
$\Omega_1^0 - \Omega_1^2$	1.1 GeV	1.0 GeV	2.3 GeV	1.6 GeV
$\Omega_1^{0,\,\ln} - \Omega_1^{2,\,\ln}$	1.8 GeV	1.0 GeV	4.6 GeV	2.0 GeV
$\Omega_1^0 - \Omega_1^3$	1.5 GeV	1.3 GeV	3.2 GeV	2.1 GeV
$\Omega_1^{0,\,\ln} - \Omega_1^{3,\,\ln}$	2.6 GeV	1.3 GeV	6.6 GeV	2.8 GeV

TABLE VII. Power correction differences extracted from the fits in Fig. 8. The slope parameter $\Omega_1^{n,\,\ln}$ is defined in Eq. (83). These values have 10% to 20% uncertainties from the choice of functional fit form.

$Q \sim m_Z$. More interestingly, both programs show logarithmic growth in Q for the power correction, as expected from our results in Sec. V A. Numerically, this growth is consistent with the form $(\ln Q)^A/Q$ found in Ref. [1], and the exponent $A \simeq 4C_A/\beta_0 \sim 1.5$ is presumably related to the exponent in Eq. (64). A more concrete comparison is difficult since the analysis in Ref. [1] effectively expands about $r = 1$, and parametrizes the extra resulting logarithmic singularity by a $\ln(\mu/\Lambda_{\rm QCD})$ factor that cancels an $\alpha_s(\mu)$.

To show the importance of resummation, we fit for the functional form of $\Omega(r,\mu_0)$. The solid lines in Fig. 8 have the full running in Eq. (64), while the dashed lines correspond to the expansion in Eq. (66). These curves were obtained following the procedure of Sec. V C, where $\Omega(r,\mu_0)$ is modeled using the three basis functions

$$\{1, r, (1-r)^{-1/4}\}, \tag{82}$$

suitable orthonormalized. The inclusion of $(1-r)^{-1/4}$ is needed to capture the (integrable) peak of $\Omega(r,\mu_0)$ at $r = 1$, though other choices $(1-r)^k$ give comparable results. We apply the fit form at $Q = 100$ GeV and use Eq. (64) to determine $\Omega(r,\mu)$ over the whole Q range.[17] To show that this framework has some predictive power, we fit $\Omega(r,\mu_0)$ using information from $n = 1$ and $n = 2$ over the whole Q range, and then extrapolate to $n = 3$.

Because we are measuring the difference $\tau_{(0,a)} - \tau_{(n,a)}$, we are relatively insensitive to the functional form of $\Omega(r,\mu_0)$ near $r = 1$. We are effectively measuring event shapes in the universality class $g_e(r) = 1 - r^n$ where

---

[17] As mentioned below Eq. (64), a more natural strategy would be to apply the fit form at $\mu_0 = 2$ GeV. Because of large range of scales in Fig. 8 resummation is always important with that choice. By using $\mu_0 = (100$ GeV$)/2$ we are using the same scale where Monte Carlos have been tuned, and we can also better highlight the difference between the full and expanded running.

$g_e(1) = 0$, and therefore our extraction of the raw power correction Ω_1^n has large uncertainties. On the other hand, the extraction of power correction differences is stable at the 10% to 20% level as the fit form is adjusted, and these differences are shown in Table VII for the basis choice in Eq. (82).

We also show the best fit values for $\Omega_1^{n,\ln}$, defined as

$$\Omega_1^{n,\ln}(\mu_0) \equiv -\int dr \, \ln(1 - r^2) \, r^n \, \Omega_1(r, \mu_0) \,, \qquad (83)$$

which is a hadronic parameter related to the slope of the expanded running in Eq. (66). We see that Pythia 8 and Herwig++ have similar power corrections Ω_1^n at $Q = 100$ GeV, but the slopes $\Omega_1^{n,\ln}$ are larger in Pythia 8, leading to larger values of Ω_1^n at $Q = 10^4$ GeV. This slope parameter is interesting since it provides an example of a hadronization effect that can only be accurately determined using data at multiple Q values. Parameters of this type presumably dominate the uncertainty one has when describing hadronization effects in high energy data using Monte Carlo models that were only tuned at much lower energies.

Finally, we remark that one strategy to extract Ω_1^n directly from these Monte Carlo programs would be to turn off the hadronization model and calculate $\langle \tau_{(n,a)} \rangle_{\text{pert}}$ from the parton shower alone. However, there is no guarantee of a one-to-one map between hadronization modeling and operator-derived power corrections. In the context of a Monte Carlo program, the perturbative parton shower is first evolved to the shower cutoff of order 1 GeV $> \Lambda_{\text{QCD}}$ before applying the hadronization model, whereas from Sec. V B the natural scale to evaluate the power correction is Qe (for the distribution) or $Qe_{\max}$ (for the first moment). For this reason, there is an ambiguous separation between perturbative parton shower evolution and nonperturbative hadronization modeling, and there is no guarantee that hadronization models by themselves will respect the renormalization group evolution of Eq. (64).[18] It would be interesting to understand to what extent parton shower evolution can mimic Eq. (64), and whether there are ways to adjust hadronization models to satisfy the renormalization group properties expected of power corrections. Ultimately, one would want to test the power correction evolution by performing event shape measurements at high Q.

VI. CONCLUSIONS

In this paper, we revisited the important issue of power corrections for e^+e^- dijet event shapes. By casting the

leading power correction in terms of matrix elements of a transverse velocity operator, we are able to robustly treat the effect of hadron masses. Depending on the measurement scheme, event shapes fall into different universality classes that share a universal power correction $\Omega_1^{g_e}$. Moreover, these nonperturbative matrix elements have perturbatively calculable anomalous dimensions, which introduce additional dependence on the scale Q of the hard collision.

Since Monte Carlo programs play such a key role in LHC data analysis, it is satisfying to see that both universality and Q-evolution are exhibited by the hadronization models of Pythia 8 and Herwig++, albeit with different choices of the nonperturbative matrix elements. An interesting difference is in their values for hadronic slope parameters that play an important role in the extrapolation to high energies of hadronization effects that are fit at low energies.

Our study motivates a reanalysis of e^+e^- event shape data with a more explicit treatment of hadron mass effects. As an exercise, we have studied the effect of including the anomalous dimension of the leading power correction on the determination of $\alpha_s(m_Z)$ from the thrust distribution. We have repeated the analysis of Ref. [30] at $N^3LL + \mathcal{O}(\alpha_s^3)$, using the same data set and procedure, but replacing the power correction to include a logarithmic slope term

$$2\,\Omega_1 \to 2\,\Omega_1 - \frac{\alpha_s(\mu_s)C_A}{\pi}\,\Omega_1^{\ln}\,\log\left(\frac{\mu_s}{2\,\text{GeV}}\right), \qquad (84)$$

where $\mu_s(\tau) \sim Q\tau$. With the current experimental data, Ω_1 and $\Omega_1^{\ln}$ are highly correlated and cannot be determined simultaneously. Therefore we plug in the estimate $\Omega_1^{\ln} = \pm 0.35$ GeV $\sim \pm\Omega_1$, and repeat the fit for $\alpha_s(m_Z)$ and Ω_1. We find that the effect of this term on $\alpha_s(m_Z)$ is ± 0.0005, which is roughly half of the total uncertainty ± 0.0011 found in Ref. [30]. For Ω_1 the effect is ∓ 0.03 GeV, which is comparable to the previous uncertainty of ± 0.05 GeV. Accounting for this additional source of uncertainty in quadrature changes the total uncertainty in this analysis from $\pm 0.0011 \to \pm 0.0012$ for $\alpha_s(m_Z)$, and from $\pm 0.05 \to \pm 0.06$ for Ω_1.

If LEP data is successfully preserved [85, 86], then one could compare different mass scheme to better separate perturbative physics from nonperturbative physics. Such studies would be interesting in their own right, but would also give additional input for tuning Monte Carlo hadronization models.

An obvious generalization is to go beyond dijet event shapes and consider shape functions for more than two Wilson lines. This is relevant not only for multijet studies at e^+e^- colliders but also for treating the beam directions in hadron colliders like the LHC. For example, the event shape N-jettiness [69] is a convenient variable to define exclusive N-jet cross sections at the LHC, and its shape function involves $2 + N$ Wilson lines. The anomalous dimension calculation for multiple Wilson lines is technically more challenging but conceptually similar to

---

[18] For example, if we were to extract Ω_1^0 from Pythia 8 by turning hadronization on and off, we would find almost no running with Q (i.e. $\Omega_1^{0,\ln} \simeq 0$).

the calculation presented here. In particular, the same $\hat{\mathcal{E}}_T(r, y, \hat{t})$ can be considered for this analysis (where here we add $\hat{t}$ in order to emphasize that rapidity y is defined with respect to the axis $\hat{t}$). On the other hand, it is not clear which aspects of universality will carry over to the multijet case, since universality of dijet power corrections relied crucially on longitudinal boost invariance.

Finally, our study sheds light on recent studies of jet substructure at the LHC. The jet shape N-subjettiness was introduced in Refs. [87, 88] (see also Ref. [89]) as a complement to the event shape N-jettiness. The ratio of 2-subjettiness to 1-subjettiness ($\tau_{2/1}$) can be used to distinguish boosted W/Z bosons from the background of ordinary quark and gluon jets. From Table I we see that 2-jettiness and thrust are closely related, and Ref. [90] used this fact to perform a precision calculation of $\tau_{2/1}$ for boosted W/Z bosons at the LHC by recycling the known resummation for thrust in $e^+ e^- \to$ hadrons. However, Table V shows that the original definitions of 2-jettiness and thrust are not in the same universality class, which explains why Ref. [90] required a value of the power correction $\Phi_1 \equiv \Omega_1^\rho$ that was roughly a factor of two bigger than the value for Ω_1^τ obtained in Refs. [29, 30]. To a good approximation, the power correction for boosted W/Z bosons generates a shift of the $\tau_{2/1}$ distribution by π times Ω_1^ρ [90], making it all the more crucial to choose the proper power correction. Thus a proper treatment of hadron masses and power corrections will be essential for precision jet substructure studies at the LHC.

Appendix A: Derivation of the Transverse Velocity Operator

In this appendix we show that the transverse velocity operator $\hat{\mathcal{E}}_T(r, y)$ can be expressed in terms of the energy-momentum tensor as in Eq. (26). Our analysis is analogous to that for $\hat{\mathcal{E}}_T(\eta)$ in Ref. [68], where it was performed for scalar and spin-1/2 hadrons, as well as that of Ref. [66]. We will carry out our proof for scalar fields.

Consider the energy-momentum tensor of a free scalar particle with mass m (we will see below that interaction terms are suppressed):

$$T^{\mu\nu} = \partial^\mu \phi \, \partial^\nu \phi - g^{\mu\nu} \mathcal{L}, \tag{A1}$$

where the plane wave expansion for the scalar field is

$$\phi(x) = \int \frac{d^3\vec{p}}{(2\pi)^3 2E_p} \left(a_{\vec{p}} e^{-i\,x\cdot p} + a_{\vec{p}}^\dagger e^{i\,x\cdot p} \right), \tag{A2}$$

where $E_p = \sqrt{p^2 + m^2}$. We will use the stationary phase approximation

$$\lim_{k\to\infty} \int dx \, f(x) \, e^{i\,k\,g(x)} \tag{A3}$$

$$= \sqrt{\frac{2\pi}{k\,|g''(x_0)|}} \, f(x_0) \, e^{i\,k\,g(x_0)} e^{i\,\frac{\pi}{4}\,\text{sign}[g''(x_0)]},$$

where $g'(x_0) = 0$. For this formula to be applicable, $g(x)$ must attain a minimum or a maximum in the range of integration.

After plugging the plane wave expansion of the free field ϕ in Eq. (A2) into the energy-momentum tensor in Eq. (A1), one can perform all the angular integrations using Eq. (A3), obtaining

$$\lim_{R\to\infty} R^3 \hat{n}_i \, T^{0i}(R, R\,v\,\hat{n}) \tag{A4}$$

$$= \lim_{R\to\infty} R \int \frac{dp\,dq\,p\,q^2}{4(2\pi)^4 E_q\,v^2} \Big(a_{\vec{p}_{\hat{n}}} a_{\vec{q}_{\hat{n}}} e^{iR(vp - E_p + vq - E_q)}$$

$$+ a_{\vec{p}_{\hat{n}}} a_{\vec{q}_{\hat{n}}}^\dagger e^{iR(vp - E_p - vq + E_q)} + (\text{h.c. and } p \leftrightarrow q) \Big),$$

where $\vec{p}_{\hat{n}} = p\,\hat{n}$ and $\vec{q}_{\hat{n}} = q\,\hat{n}$. The p and q integrals can be performed, again using Eq. (A3), to yield

$$\lim_{R\to\infty} R^3 \hat{n}_i \, T^{0i}(R, v\,R\,\hat{n})$$

$$= \frac{1}{4(2\pi)^3} \frac{m^3 v}{(1-v^2)^{\frac{5}{2}}} \left(a_{\tilde{p}} a_{\tilde{p}}^\dagger + a_{\tilde{p}}^\dagger a_{\tilde{p}} \right), \tag{A5}$$

where $\tilde{p} = \frac{mv}{\sqrt{1-v^2}}\,\hat{n}$. Note that terms involving two creation or two annihilation operators drop out, since they vanish as $1/R$ when integrated against any function of v (in particular our $g_e(r)$ in Eq. (36)). At this point we can also see why interaction terms in the energy-momentum tensor can be neglected. Such terms involve additional fields and therefore additional integrations when they are expanded in plane waves. These additional integrals can be performed using the stationary phase approximation and vanish as $R \to \infty$ due to the presence of additional powers of $1/R$.

After normal ordering, Eq. (A5) can be written as

$$\lim_{R\to\infty} R^3 \hat{n}_i \, T^{0i}(R, v\,R\,\hat{n}) \tag{A6}$$

$$= \int \frac{\mathrm{d}^3\vec{p}}{(2\pi)^3 2E_p} \, a_p^\dagger \, a_p \, \frac{E_p}{v} \, \delta\Big(v - \frac{|\vec{p}|}{E_p}\Big) \delta^2(\hat{p} - \hat{n}) \,.$$

Using the fact that $E_p = (p^\perp \cosh\eta)/v$ and

$$\int_0^{2\pi} \mathrm{d}\phi \, \delta^2(\hat{p} - \hat{n}) = \cosh^2\eta \, \delta(\eta - \eta_p) \,, \qquad (A7)$$

we obtain the operator

$$\hat{\mathcal{E}}_T(v,\eta) = \frac{v^2}{\cosh^3\eta} \lim_{R\to\infty} R^3 \int_0^{2\pi} \mathrm{d}\phi \, \hat{n}_i \, T^{0i}(R, R\,v\,\hat{n}), \quad (A8)$$

which is differential in velocity and pseudo-rapidity and satisfies:

$$\hat{\mathcal{E}}_T(v,\eta)|X\rangle = \sum_{i\in X} p_i^\perp \delta(v - v_i) \, \delta(\eta - \eta_i) \, |X\rangle \,. \qquad (A9)$$

Note that if we integrate this operator over $0 < v < 1$, we recover the expression in Ref. [66] for the energy flow operator $\hat{\mathcal{E}}_T(\eta)$.

Finally, to obtain from $\hat{\mathcal{E}}_T(v,\eta)$ the desired $\hat{\mathcal{E}}_T(r,y)$ that satisfies Eq. (25), one needs to multiply by the Jacobian factor

$$\frac{\partial(v,\eta)}{\partial(r,y)} = \frac{\mathrm{sech}^2 y}{r} \,, \qquad (A10)$$

and include a factor $1/r$ to convert $p^\perp$ to $m^\perp$, yielding

$$\hat{\mathcal{E}}_T(r,y) = \frac{\mathrm{sech}^2 y}{r^2} \, \hat{\mathcal{E}}_T\big(v(r,y),\eta(r,y)\big) \,, \qquad (A11)$$

which agrees with Eq. (26).

Appendix B: Renormalon Computation for Generic Event Shape

Here we show that the definition $\delta_e(R,\mu) = (c_e/c_{e'})\delta_{e'}(R,\mu)$ in Eq. (58) yields a perturbative cross section $\tilde{\sigma}_e(x)$ in Eq. (56) that is independent of the leading $\Lambda_{\rm QCD}$ renormalon when probed by a standard fermion bubble chain. Since the renormalon cancels between the $\overline{\rm MS}$ series $\hat{\sigma}_e(x)$ and $\Omega_1^e(\mu)$, this implies that $\Omega_1^e(R,\mu)$ is also free of the $\Lambda_{\rm QCD}$ renormalon.

The $\Lambda_{\rm QCD}$ renormalon corresponds to a $u = 1/2$ pole in the Borel transform. For a function $f(\alpha_s)$ that is an infinite series in $\alpha_s(\mu)$, the Borel transform $B[f](u)$ is obtained by replacing

$$\Big(\frac{\beta_0 \alpha_s(\mu)}{4\pi}\Big)^{n+1} \to \frac{u^n}{n!} \,. \qquad (B1)$$

Following Ref. [62] we make use of the fact that the perturbative soft function carries the leading renormalon, and hence carry out our computation for $S_e^{\rm pert}(x,\mu)$

rather than the cross section $\hat{\sigma}(x)$.[19] Since the soft function obeys non-Abelian exponentiation [91, 92] it is useful to write the perturbative scheme change in Eq. (56) as

$$\ln \tilde{S}_e^{\rm pert}(x,\mu) = \ln S_e^{\rm pert}(x,\mu) - ix\,\delta_e(R,\mu) \,, \qquad (B2)$$

and then demonstrate that $\ln \tilde{S}_e^{\rm pert}(x,\mu)$ does not have a $u = 1/2$ pole.

The use of the soft function allows us to perform the bubble chain analysis for an arbitrary event shape specified by $f_e(r,y)$ and Eq. (9). To study the first contribution to the $u = 1/2$ pole, we can work in $d = 4$ dimensions and we only need to dress a single real gluon with a bubble chain. We parametrize the gluon phase space with $\vec{p}_\perp$ and y,

$$\frac{\mathrm{d}^3\vec{p}}{(2\pi)^3 2E_p} = \frac{\mathrm{d}y}{4\pi} \frac{\mathrm{d}^2\vec{p}_\perp}{(2\pi)^2} \,. \qquad (B3)$$

Since the final state gluon is on-shell, we have $r = 1$. For the event shape e, the Fourier transform gives

$$\int \mathrm{d}e \, e^{-iexQ} \, \delta\Big(e - \frac{1}{Q} p_\perp f_e(1,y)\Big) = e^{-ix\,p_\perp f_e(1,y)} \,. \qquad (B4)$$

Taking the sum of all dressed real radiation diagrams with a single gluon and swapping $n_f \to -3\beta_0/2$, we find the Borel transform

$$B\big[\ln S_e^{\rm bubbles}(x,\mu)\big](u) \qquad\qquad (B5)$$

$$= \frac{8C_F\big(\mu^2 e^{5/3}\big)^u}{\beta_0 \Gamma(1+u)\Gamma(1-u)} \int_{-\infty}^{+\infty} \mathrm{d}y \int_0^\infty \mathrm{d}p_\perp \, p_\perp^{-1-2u} \, e^{-ix\,p_\perp f_e(1,y)}$$

$$= \frac{8C_F\big(\mu^2 e^{5/3}\big)^u}{\beta_0 \Gamma(1+u)\Gamma(1-u)} \int_{-\infty}^{+\infty} \mathrm{d}y \, f_e(1,y)^{2u} \int_0^\infty \mathrm{d}h \, h^{-1-2u} e^{-ixh}$$

$$= \frac{8C_F\big(\mu^2 e^{5/3}\big)^u}{\beta_0 \Gamma(1+u)\Gamma(1-u)} \Gamma(-2u)(ix)^{2u} \int_{-\infty}^{+\infty} \mathrm{d}y \, f_e(1,y)^{2u} \,.$$

Here $\beta_0 = 11C_A/3 - 2n_f/3$, and in the second equality we used the change of variables $h = p_\perp f_e(1,y)$. Expanding about $u = 1/2$ and using $\int \mathrm{d}y \, f_e(1,y) = c_e$, we arrive at the final expression for the $u = 1/2$ pole

$$B\big[\ln S_e^{\rm bubbles}(x,\mu)\big](u) = c_e \frac{8C_F e^{5/6}}{\pi\beta_0(u - \frac{1}{2})} \, (ix\mu) \,. \qquad (B6)$$

Here (ix) corresponds to the $\delta'(\ell)$ present in Eq. (16).

Using Eq. (B6) we can compute the Borel transform of the subtraction series $\delta_{e'}(R,\mu)$ for the reference event shape e', which is defined by Eq. (58). We find

$$B\big[\delta_{e'}(R,\mu)\big](u) = c_{e'} \frac{8C_F e^{5/6}}{\pi\beta_0(u - \frac{1}{2})} \, \mu \,. \qquad (B7)$$

---

[19] Note that x is a dimensionless variable in $\hat{\sigma}(x)$ but is a variable with mass dimension -1 in $S_{\rm pert}^e(x,\mu)$.

Finally, computing the leading renormalon ambiguity in $\ln \tilde{S}_{\text{pert}}^e$, using Eq. (58) to define $\delta_e(R, \mu)$, we find

$$B\big[\ln \tilde{S}_e^{\text{pert}}(x, \mu)\big](u) \qquad (B8)$$

$$= B\big[\ln S_e^{\text{pert}}(x, \mu)\big](u) - ix\, B\big[\delta_e(R, \mu)\big](u)$$

$$= B\big[\ln S_e^{\text{pert}}(x, \mu)\big](u) - ix\, \frac{c_e}{c_{e'}}\, B\big[\delta_{e'}(R, \mu)\big](u)$$

$$= \frac{0}{u - \frac{1}{2}},$$

as promised. Note the importance of using the same scale μ for the perturbative soft function $S_e^{\text{pert}}(x, \mu)$ and its subtractions $\delta_e(R, \mu)$.

As a final comment, we remark that the renormalon analysis in this appendix takes $r = 1$ and hence does not fully probe infrared effects that depend on hadron masses.

Appendix C: One-Loop Anomalous Dimension

In this appendix we provide details on the calculation which yields the anomalous dimension formula in Eq. (61). The integrals involved in determining the one-loop anomalous dimension of $\Omega_1(r, \mu)$ from Figs. 4–7 are somewhat different from the phase space integrals for QCD gluons attached to eikonal lines, which occur for the leading power perturbative soft function calculation. In particular the amplitudes are similar to those occurring in recent two-loop soft function calculations [93–95], but a different measurement is made.

As explained in Sec. V, one of the cut gluons corresponds to a massive adjoint source field, and $\hat{\mathcal{E}}_T(r, y)$ acts on this object. We will call the momentum of this source q^μ, where $q^2 = m^2 \neq 0$. The remaining gluon lines are standard massless QCD gluons, and we will denote the momentum of virtual loop integrals by k, and the momenta of real gluon radiation by p, where $p^2 = 0$.

The phase space integral over q for the source is completely fixed by the measurement, up to one trivial angular integral for ϕ_q in the transverse plane. Taking the three phase space variables to be q^+, q^-, and ϕ_q the former two are fixed by the δ-functions from Eq. (25):

$$m_q^\perp \delta(r - r_q)\, \delta(y - y_q) \qquad (C1)$$

$$= m_q^\perp \frac{2\, m^2 r}{(1 - r^2)^2} \delta\Big(q^+ - \frac{me^y}{\sqrt{1-r^2}}\Big)\delta\Big(q^- - \frac{me^{-y}}{\sqrt{1-r^2}}\Big),$$

where $m_q^\perp = \sqrt{q_\perp^2 + m^2}$, $r_q = q_\perp / m_q^\perp$, and $y_q = 1/2 \ln(q^+/q^-)$. For notational convenience we define an object $\hat{\Phi}(r, y)$ that contains common factors associated with the source that appear in all Feynman diagrams,

$$\hat{\Phi}(r, y) = \frac{16\pi\alpha_s C_F}{(2\pi)^n} \int \frac{\mathrm{d}^n \vec{q}}{2E_q} \frac{m_q^\perp \delta(r - r_q)\, \delta(y - y_q)}{q^+ q^-}\,, \quad (C2)$$

where $n = d - 1 = 3 - 2\epsilon$. Here $\hat{\Phi}(r, y)$ should be considered to be an operator that can act on additional q^+ and

q^- dependence in loop and phase space integrals, and which replaces $q^\pm$ by the functions of m, r, y occurring in the δ-functions in Eq. (C1). $\hat{\Phi}(r, y)$ is normalized so that acting on unity with $n = 3$ the integral in Eq. (C2) yields the tree level result in Eq. (60).

The general strategy to compute the anomalous dimension is to reduce each graph to a set of master integrals. We will always partial fraction eikonal propagators and shift numerators to obtain a set of integrals that involve only one p^+ (k^+) and/or one p^- (k^-) in a denominator. To regulate potential IR singularities we shift the eikonal propagators by taking $k^\pm \to k^\pm + \Delta_{n,\bar{n}}$ or $p^\pm \to p^\pm + \Delta_{n,\bar{n}}$. We will treat the $\Delta_{n,\bar{n}}$ as infinitesimal IR regulators, which are expanded whenever possible.

We start with graphs which involve independent emission of gluons in Figs. 5 and 6. A useful identity between real emission phase space and virtual integrals is

$$I_1(A, B) = \tilde{\mu}^{2\epsilon} \int \frac{\mathrm{d}^{d-1}\vec{p}}{2|\vec{p}|(2\pi)^{d-1}} \frac{1}{(p^+ + A)} \frac{1}{(p^- + B)}$$

$$= i\, \tilde{\mu}^{2\epsilon} \int \frac{\mathrm{d}^d k}{(2\pi)^d} \frac{1}{(k^+ + A)} \frac{1}{(k^- + B)} \frac{1}{k^2 + i0}$$

$$= \frac{1}{(4\pi)^2} \Gamma(\epsilon)^2 \Gamma(1 - \epsilon) \Big(e^{\gamma_E} \frac{\mu^2}{A\,B}\Big)^\epsilon, \qquad (C3)$$

where $\tilde{\mu} = \mu e^{\gamma_E}/(4\pi)$.[20] Using Eq. (C3) it is easy to determine that the purely Abelian terms proportional to C_F^2 vanish (virtual graphs cancel real radiation graphs). In addition in the sum of non-Abelian contributions from the graphs in Fig. 6, there are no IR divergences regulated by ϵ or $\Delta_{n,\bar{n}}$, so all $1/\epsilon$'s correspond to UV divergences. The result for these non-Abelian independent emission contributions is

$$M_{\text{ie}}^{\text{EFT}} = -8\pi\alpha_s C_A \hat{\Phi}(r, y)\, I_1(q^+, q^-) \qquad (C4)$$

$$= -\frac{C_A \alpha_s}{2\pi} \hat{\Phi}(r, y)\Big[\frac{1}{\epsilon^2} - \frac{1}{\epsilon} \ln\Big(\frac{q^+ q^-}{\mu^2}\Big) + \frac{\pi^2}{4}$$

$$+ \frac{1}{2} \ln^2 \Big(\frac{q^+ q^-}{\mu^2}\Big)\Big].$$

Note that we refer to the results of this section as effective field theory (EFT) contributions since we are performing calculations in a theory where the soft perturbative scale ($\mu_S \sim Qe$) has been integrated out.

Graphs involving the triple gluon vertex are more involved. Here individual virtual radiation graphs have an imaginary part, which arises from the fact that $q^2 = m^2 > 0$ while all virtual particles have massless propagators. Nevertheless the virtual diagrams can always be paired with a complex conjugate so one only

---

[20] Eq. (C3) has IR divergences regulated by ϵ for either A or B zero (strictly speaking UV divergences cancel IR divergences in pure dimensional regularization, and the integral is zero). The equality between real and virtual integrals is still valid for these cases.

needs the real parts. To determine the anomalous dimension for $\Omega_1(r,\mu)$, we only need the UV-divergent terms. The finite terms would be necessary for the matching computation of $d_1^e(r)$ in Eq. (71), which is not our goal here. We will therefore focus on graphs which contain $1/\epsilon$ UV divergences and μ dependence. The μ-dependent terms will be needed for App. D.

It is straightforward to verify that the sum of double cut vacuum polarization graphs in Fig. 4 does not have a $1/\epsilon$ UV divergence. They also do not require ϵ to regulate IR divergences, and hence have no explicit μ dependence. Thus they do not contribute to our calculation here.

The remaining triple gluon vertex diagrams shown in Fig. 7 involve single cut virtual graphs and double cut real emission graphs. The only required UV divergent and μ-dependent loop integral is

$$
I_2(A, q^+, m) \tag{C5}
$$
$$
= \mathrm{Re}\left[i\,\tilde{\mu}^{2\epsilon}\int\frac{\mathrm{d}^d k}{(2\pi)^d}\frac{1}{(k^+ + A)}\frac{1}{k^2 + i0}\frac{1}{(k-q)^2 + i0}\right]
$$
$$
= \frac{-1}{(4\pi)^2}\Gamma(\epsilon)\cos(\epsilon\pi)\left(e^{\gamma_E}\frac{\mu^2}{m^2}\right)^\epsilon\int_0^1 \mathrm{d}x\,\frac{[x(1-x)]^{-\epsilon}}{A + xq^+}.
$$

The result is IR safe for all the cases we need ($A \neq 0$ and $A \neq -q^+$), yielding

$$
I_2(A, q^+, m) = -\frac{1}{(4\pi)^2 q^+}\left[\frac{1}{\epsilon} - 2\ln\left(\frac{m}{\mu}\right)\right]\ln\left(1 + \frac{q^+}{A}\right)
$$
$$
+ \ldots, \tag{C6}
$$

where the $+\ldots$ refers to UV finite and μ-independent terms. The real radiation master integral is

$$
I_3(A, q^+, m) = \tilde{\mu}^{2\epsilon}\int\frac{\mathrm{d}^{d-1}\vec{p}}{2|\vec{p}|(2\pi)^{d-1}}\frac{1}{(p^+ + A)}\frac{1}{(2p\cdot q + m^2)}
$$
$$
= \frac{\Gamma(\epsilon)}{(4\pi)^2}\left(e^{\gamma_E}\frac{\mu^2}{m^2}\right)^\epsilon\int_0^\infty \mathrm{d}x\,\frac{[x(1+x)]^{-\epsilon}}{A + xq^+},
$$

which is IR safe for all cases we need ($A \neq 0$), yielding

$$
I_3(A, q^+, m) = \frac{1}{(4\pi)^2}\frac{1}{q^+}\left\{\frac{1}{2\epsilon^2} - \frac{1}{\epsilon}\ln\left(\frac{m}{\mu}\right)\right. \tag{C7}
$$
$$
\left. + \ln^2\left(\frac{m}{\mu}\right) - \ln\left(\frac{A}{q^+}\right)\left[\frac{1}{\epsilon} - 2\ln\left(\frac{m}{\mu}\right)\right]\right\} + \ldots.
$$

Here all $1/\epsilon$ poles are UV divergences, and again the $+\ldots$ represent UV finite and μ-independent terms. We can always group terms with IR divergences as $\Delta_{n,\bar{n}} \to 0$ into the IR finite combination

$$
I_{23}(q^+, m) \equiv I_3(\Delta, q^+, m) + I_2(\Delta, q^+, m). \tag{C8}
$$

The result is independent of Δ

$$
I_{23}(q^+, m^2) = \frac{1}{(4\pi)^2}\frac{1}{q^+}\left[\frac{1}{2\epsilon^2} - \frac{1}{\epsilon}\ln\left(\frac{m}{\mu}\right) + \ln^2\left(\frac{m}{\mu}\right)\right.
$$

$$
+ \ldots\bigg]. \tag{C9}
$$

The sum of all diagrams in Fig. 7 is

$$
M_{\mathrm{ggg}}^{\mathrm{EFT}} = 4\pi\alpha_s C_A \hat{\Phi}(r, y)\Big[q^- I_{23}(q^-, m) + q^+ I_{23}(q^+, m)
$$
$$
+ q^- I_3(q^-, q^-, m) + q^+ I_3(q^+, q^+, m) + \ldots\Big]
$$
$$
= \frac{C_A\,\alpha_s}{2\pi}\hat{\Phi}(r, y)\left[\frac{1}{\epsilon^2} - \frac{2}{\epsilon}\ln\left(\frac{m}{\mu}\right) + 2\ln^2\left(\frac{m}{\mu}\right) + \ldots\right]. \tag{C10}
$$

Finally, adding all one-loop diagrams, the $1/\epsilon^2$ terms vanish, and we get the following final result for the UV-divergent and μ-dependent terms from the graphs in Fig. 7:

$$
M_{\mathrm{1loop}}^{\mathrm{EFT}} = \hat{\Phi}(r, y)\frac{\alpha_s C_A}{\pi}\ln\left(\frac{q^+ q^-}{m^2}\right)\left[\frac{1}{2\epsilon} - \ln\left(\frac{m}{\mu}\right)\right]
$$
$$
+ \ldots. \tag{C11}
$$

Due to $\hat{\Phi}(r, y)$, we have $\ln(q^+ q^-/m^2) = -\ln(1-r^2)$, and this result reproduces the $1/\epsilon$ term shown in Eq. (61).[21]

The expression in Eq. (C11) corresponds to a bare result in the EFT. The renormalized result $\bar{M}_{\mathrm{1loop}}^{\mathrm{EFT}}$ is simply obtained in minimal subtraction by canceling the UV-singularity with a counterterm $Z(r, \mu, \epsilon)$, and will be used in App. D. For that purpose, we also note that the sum of independent emission and triple-gluon virtual graphs is UV finite, so the entire contribution shown in Eq. (C11) comes from the real emission diagrams.

Appendix D: One-Loop Matching for Thrust

In this appendix we consider the one-loop matching computation that determines $C_1^e(\ell, r, \mu)$ in Eq. (68) for the case where e is thrust. Only μ-dependent terms will be considered since our goal is to see how the function $\mathrm{d}/\mathrm{d}\ell[1/\mu(\mu/\ell)_+]$ arises from the matching computation.

---

[21] This same result can also be obtained setting $\Delta_{n,\bar{n}} = 0$ from the start and using dimensional regularization for the IR divergences. In this case we would use

$$
I_2(0, q^+, m^2) = -I_2(-q^+, q^+, m^2)
$$
$$
= \frac{-1}{(4\pi)^2}\frac{\Gamma(\epsilon)\Gamma(-\epsilon)\Gamma(1-\epsilon)}{\Gamma(1-2\epsilon)}\frac{1}{q^+}\cos(\epsilon\pi)\left(e^{\gamma_E}\frac{\mu^2}{m^2}\right)^\epsilon,
$$

and

$$
I_3(0, q^+, m) = -I_3(q^+, q^+, m) = \frac{\Gamma(2\epsilon)\Gamma(-\epsilon)}{(4\pi)^2}\frac{1}{q^+}\left(e^{\gamma_E}\frac{\mu^2}{m^2}\right)^\epsilon
$$
$$
= \frac{-1}{(4\pi)^2}\frac{1}{q^+}\left[\frac{1}{2\epsilon^2} - \frac{1}{\epsilon}\ln\left(\frac{m}{\mu}\right) + \ln^2\left(\frac{m}{\mu}\right) + \frac{5\pi^2}{24}\right].
$$

In this case the sum of all diagrams is again IR finite and again reproduces Eq. (C11).

A matching computation is performed by considering the difference of renormalized full theory and renormalized effective theory matrix elements, which are calculated with precisely the same infrared regulator(s). For our computation the full theory corresponds to matrix elements of the soft function. For an event shape e, it is

$$S_e(\ell) = \langle 0 | \overline{Y}_{\bar{n}}^\dagger Y_n^\dagger \delta(\ell - Q\hat{e}) Y_n \overline{Y}_{\bar{n}} | 0 \rangle \tag{D1}$$
$$= \sum_X \langle 0 | \overline{Y}_{\bar{n}}^\dagger Y_n^\dagger | X \rangle \delta[\ell - Qe(X)] \langle X | Y_n \overline{Y}_{\bar{n}} | 0 \rangle,$$

where the sum is over all possible intermediate states and includes also integrals over phase space. The EFT for this computation corresponds to the field theory obtained by integrating out the scale ℓ, and involves matrix elements like $\Omega_1(r)$ in Eq. (32). In this language the anomalous dimension calculation in App. C corresponded to finding the UV counterterm for the $\Omega_1(r)$ matrix element in the EFT. For a matching computation that only considers μ-dependent terms, the required renormalized EFT matrix element corresponds to the $\ln(m/\mu)$ term in Eq. (C11). This result is independent of the event shape e, in contrast to the $d_1^e(r)$ term in Eq. (71) which is event shape specific.

Here we perform a computation of the corresponding full theory matrix elements in Eq. (D1) with the same IR regulators, which includes the use of the source $J^{\mu A}$ field of momentum q^μ where $q^2 = m^2$. Since some parts of this computation depend on the choice of e, we will restrict ourselves to a computation for thrust. We will use the same notation as App. C for loop and phase space integrals. Unlike the EFT, the full theory results involve hierarchical scales, $\ell \gg q^\mu \sim m$, and hence the final full theory result must be expanded before subtracting the EFT result.

At the order of our calculation, we can split the $\sum_X$ in Eq. (D1) into terms with no source term (which gives rise to the purely perturbative soft function), and terms with one source term. In general the expansion $\ell \gg q$ should only be performed after carrying out the full theory loop and phase space integrals, but in cases where the expansion and integration commute we can do them in either order. One example where this is useful is in the measurement function $\delta(\ell - Qe(X))$. Denoting by $e(q)$ the contribution from the source, and $e(p_i)$ the contribution from all other real radiation gluons we can expand $\ell \sim Qe(p_i) \gg Qe(q)$, and keeping the first two terms

$$\delta[\ell - Qe(p_i) - Qe(q)] \tag{D2}$$
$$= \delta[\ell - Qe(p_i)] - Qe(q)\, \delta'[\ell - Qe(p_i)].$$

For the corresponding terms in $S_e(\ell)$ this yields

$$S_e(\ell) = S_e^{\mathrm{pert}}(e) - \frac{\mathrm{d}}{\mathrm{d}\ell} \sum_{\{p_i\}, q} Qe(q)\, \delta[\ell - Qe(p_i)] \tag{D3}$$
$$\times \langle 0 | \overline{Y}_{\bar{n}}^\dagger Y_n^\dagger | p_i, q \rangle \langle p_i, q | Y_n \overline{Y}_{\bar{n}} | 0 \rangle.$$

The first term corresponds to the leading power perturbative soft function and the second term provides the full

theory contribution to the matching we are interested in. The analog of Eq. (D2) for the EFT computation is

$$\delta[\ell - Qe(p_i) - Qe(q)] = \delta(\ell) - \delta'(\ell)\,[Qe(q) + Qe(p_i)], \tag{D4}$$

where the term $Qe(p_i)$ is scaleless and vanishes. From this result we see that the EFT contribution to the matching is proportional to $-\delta'(\ell)$.

It is easy to check that the matching is simple for an Abelian theory. Due to the exponentiation and factorization properties of the Abelian eikonal matrix elements, we obtain

$$-\sum \langle 0 | \overline{Y}_{\bar{n}}^\dagger Y_n^\dagger | p_i, q \rangle \delta'[\ell - Qe(p_i)]\, Qe(q) \langle p_i, q | Y_n \overline{Y}_{\bar{n}} | 0 \rangle$$
$$= -\frac{\mathrm{d}}{\mathrm{d}\ell} S_e^{\mathrm{pert}}(\ell) \langle 0 | \overline{Y}_{\bar{n}}^\dagger Y_n^\dagger (Q\hat{e}) Y_n \overline{Y}_{\bar{n}} | 0 \rangle$$
$$= -\frac{\mathrm{d}}{\mathrm{d}\ell} S_e^{\mathrm{pert}}(\ell)\, \Omega_1^e\,. \tag{D5}$$

This result holds even if we consider including more than one source term. In Ref. [30] it was assumed that Eq. (D5) also encoded all non-Abelian contributions. While these non-Abelian contributions are indeed present, Eq. (71) implies that in general there are additional non-Abelian corrections from the $+$-function and $d_1^e(r)$ terms. The flaw in the argument in Appendix B of Ref. [30] is that the dimension-1 operator $\hat{\mathcal{E}}_T(\eta)$ is not unique, since there exists an entire family of operators $\hat{\mathcal{E}}_T(y, r)$ parametrized by r.

To carry out the full non-Abelian calculation for the second term in Eq. (D3), we use Eqs. (25) and (27) to decompose $Qe(q)$ and write the full amplitude as

$$A_\tau^{\mathrm{Full}}(\ell) = \int \mathrm{d}r\, \mathrm{d}y\, f_\tau(r, y) M_\tau^{\mathrm{Full}}(\ell, r, y)\,. \tag{D6}$$

Results for $M_\tau^{\mathrm{Full}}(\ell, r, y)$ can then be compared directly to the analogous results for $-M^{\mathrm{EFT}}(r, y)\delta'(\ell)$ obtained with various M^{EFT} results from App. C. Here M_τ^{Full} still depends on the thrust event shape because it contains $\delta(\ell - Qe(p_i))$.

The computation with one source and no additional gluons is very simple, and we find

$$M_{\mathrm{tree}}^{\mathrm{Full}} = -\hat{\Phi}(r, y)\, \delta'(\ell)\,, \tag{D7}$$

where $\hat{\Phi}(r, y)$ is given in Eq. (C2). Next consider the computation for thrust at one loop. One performs the master-integral decomposition in the same way as for the anomalous dimension computation. The sum of all full theory virtual diagrams is UV finite and μ-independent (once one performs the usual QCD renormalization). In fact the sum of diagrams involving a virtual gluon are identical in the full and EFT computations, and hence these contributions cancel when subtracting to determine the matching.

Thus we only need master integrals involving full theory diagrams with real radiation to complete the calculation. For these contributions only two new master integrals are required to compute the μ-dependent pieces.

For the thrust measurement on the real radiation gluon we will use the short-hand notation

$$\mathcal{M}_\tau(\ell, p^\pm) \equiv -\frac{\mathrm{d}}{\mathrm{d}\ell}\Big[\delta(\ell - p^+)\theta(p^- - p^+) \tag{D8}$$

$$+ \delta(\ell - p^-)\theta(p^+ - p^-)\Big],$$

and to expand the master integrals with $q \ll \ell$ we will use the identity

$$\frac{x^\epsilon}{x + \delta} = \Big[\frac{1}{x}\Big]_+ - \delta(x)\,\ln(\delta) + \epsilon\Big[\frac{\ln(x)}{x}\Big]_+ \tag{D9}$$

$$- \epsilon\,\delta(x)\Big(\frac{1}{2}\ln^2\delta + \frac{\pi^2}{6}\Big) + \mathcal{O}(\epsilon^2, \delta).$$

The first master integral shows up in the independent emission diagrams of Fig. 6 and when expanded for $q \ll \ell$ gives

$$\tilde{\mu}^{2\epsilon}\int\frac{\mathrm{d}^{d-1}\vec{p}}{2|\vec{p}|(2\pi)^{d-1}}\frac{1}{p^+ + A}\frac{1}{p^- + B}\,\mathcal{M}_\tau(\ell, p^\pm) \tag{D10}$$

$$= \frac{-1}{(4\pi)^2}\frac{\mathrm{d}}{\mathrm{d}\ell}\Big\{\frac{1}{\epsilon}\Big[\frac{2}{\mu}\Big(\frac{\mu}{\ell}\Big)_+ - \delta(\ell)\ln\Big(\frac{AB}{\mu^2}\Big)\Big]$$

$$- \frac{4}{\mu}\Big[\frac{\mu}{\ell}\ln\Big(\frac{\mu}{\ell}\Big)\Big]_+ + \delta(\ell)\Big[\ln^2\Big(\frac{A}{\mu}\Big) + \ln^2\Big(\frac{B}{\mu}\Big) + \frac{2\pi^2}{3}\Big]\Big\}.$$

The second master integral appears in the double cut graphs involving the triple gluon vertex in Fig. 7, and when expanded for $q \ll \ell$ reads

$$\tilde{\mu}^{2\epsilon}\int\frac{\mathrm{d}^{d-1}\vec{p}}{2|\vec{p}|(2\pi)^{d-1}}\frac{1}{p^+ + A}\frac{1}{2p\cdot q + m^2}\,\mathcal{M}_\tau(\ell, p^\pm) =$$

$$\frac{-1}{(4\pi)^2}\frac{1}{q^+}\frac{\mathrm{d}}{\mathrm{d}\ell}\Big\{\Big[\frac{1}{\epsilon} - \ln\Big(\frac{m^2}{q^{+2}}\Big)\Big]\Big[\frac{1}{\mu}\Big(\frac{\mu}{\ell}\Big)_+ - \delta(\ell)\ln\Big(\frac{A}{\mu}\Big)\Big]$$

$$- \frac{2}{\mu}\Big[\frac{\mu}{\ell}\ln\Big(\frac{\mu}{\ell}\Big)\Big]_+ + \delta(\ell)\ln^2\Big(\frac{A}{\mu}\Big)\Big\} + \ldots, \tag{D11}$$

where the omitted terms in the $+\ldots$ are μ-independent and UV-finite.

Adding up all the μ-dependent full theory (real radiation) diagrams we find

$$M_{\text{1loop}}^{\text{Full}}(r, y) = \hat{\Phi}(r, y)\frac{C_A\alpha_s}{\pi}\ln(1 - r^2)\Big\{\frac{\mathrm{d}}{\mathrm{d}\ell}\frac{1}{\mu}\Big[\frac{\mu}{\ell}\Big]_+$$

$$- \delta'(\ell)\ln\Big(\frac{m}{\mu}\Big)\Big\} + \ldots. \tag{D12}$$

Note that $\mu\,\mathrm{d}/\mathrm{d}\mu\, M_{\text{1loop}}^{\text{Full}}(r, y) = 0$ since the two contributions cancel each other. This is consistent with the fact that there was no UV or IR divergence regulated by ϵ. We still refer to them as μ-dependent terms since they have different functional dependence on ℓ. In Eq. (D12) μ is simply a place holder scale for splitting the result into $+$-function and δ-function terms. For the corresponding EFT result, using Eq. (C11) to get the sum of renormalized diagrams, we have

$$-\delta'(\ell)\bar{M}_{\text{1loop}}^{\text{EFT}} = -\delta'(\ell)\hat{\Phi}(r, y)\frac{C_A\alpha_s}{\pi}\ln(1 - r^2)\ln\Big(\frac{m}{\mu}\Big)$$

$$+ \cdots. \tag{D13}$$

When we subtract Eq. (D13) from Eq. (D12) we are left with only the μ-dependent $+$-function term. Identifying $\int\mathrm{d}r\,\mathrm{d}y\,f_\tau(r, y)\hat{\Phi}(r, y) = \Omega_1^\tau$, this reproduces the μ-dependent term in the matching result given in Eq. (71).

[1] G. P. Salam and D. Wicke, JHEP **05**, 061 (2001), arXiv:hep-ph/0102343.

[2] C. Lee and G. Sterman, Phys. Rev. **D75**, 014022 (2007), hep-ph/0611061.

[3] G. Hanson, G. Abrams, A. Boyarski, M. Breidenbach, F. Bulos, *et al.*, Phys.Rev.Lett. **35**, 1609 (1975).

[4] S. Bethke, Eur. Phys. J. **C64**, 689 (2009), arXiv:0908.1135 [hep-ph].

[5] A. Buckley, H. Hoeth, H. Lacker, H. Schulz, and J. E. von Seggern, Eur.Phys.J. **C65**, 331 (2010), arXiv:0907.2973 [hep-ph].

[6] A. Abdesselam, E. B. Kuutmann, U. Bitenc, G. Brooijmans, J. Butterworth, *et al.*, Eur.Phys.J. **C71**, 1661 (2011), arXiv:1012.5412 [hep-ph].

[7] A. Altheimer, S. Arora, L. Asquith, G. Brooijmans, J. Butterworth, *et al.*, J.Phys.G **G39**, 063001 (2012), arXiv:1201.0008 [hep-ph].

[8] Y. L. Dokshitzer and B. Webber, Phys.Lett. **B404**, 321 (1997), arXiv:hep-ph/9704298 [hep-ph].

[9] E. Farhi, Phys. Rev. Lett. **39**, 1587 (1977).

[10] G. Parisi, Phys.Lett. **B74**, 65 (1978).

[11] J. F. Donoghue, F. Low, and S.-Y. Pi, Phys.Rev. **D20**, 2759 (1979).

[12] L. Clavelli, Phys.Lett. **B85**, 111 (1979).

[13] T. Chandramohan and L. Clavelli, Nucl.Phys. **B184**, 365 (1981).

[14] L. Clavelli and D. Wyler, Phys.Lett. **B103**, 383 (1981).

[15] P. E. Rakow and B. Webber, Nucl.Phys. **B191**, 63 (1981).

[16] C. F. Berger, T. Kúcs, and G. Sterman, Phys. Rev. D **68**, 014012 (2003), arXiv:hep-ph/0303051.

[17] R. K. Ellis, D. A. Ross, and A. E. Terrano, Nucl. Phys. **B178**, 421 (1981).

[18] S. Catani and M. H. Seymour, Phys. Lett. **B378**, 287 (1996), arXiv:hep-ph/9602277.

[19] S. Catani and M. H. Seymour, Nucl. Phys. **B485**, 291 (1997), arXiv:hep-ph/9605323.

[20] A. Gehrmann-De Ridder, T. Gehrmann, E. W. N. Glover, and G. Heinrich, Phys. Rev. Lett. **99**, 132002 (2007), arXiv:0707.1285 [hep-ph].

[21] A. Gehrmann-De Ridder, T. Gehrmann, E. W. N. Glover,

and G. Heinrich, JHEP **12**, 094 (2007), arXiv:0711.4711 [hep-ph].

[22] S. Weinzierl, Phys. Rev. Lett. **101**, 162001 (2008), arXiv:0807.3241 [hep-ph].

[23] S. Weinzierl, JHEP **06**, 041 (2009), arXiv:0904.1077 [hep-ph].

[24] T. Becher and M. D. Schwartz, JHEP **07**, 034 (2008), arXiv:0803.0342 [hep-ph].

[25] Y.-T. Chien and M. D. Schwartz, JHEP **08**, 058 (2010), arXiv:1005.1644 [Unknown].

[26] J.-y. Chiu, A. Jain, D. Neill, and I. Z. Rothstein, Phys.Rev.Lett. **108**, 151601 (2012), arXiv:1104.0881 [hep-ph].

[27] T. Becher, G. Bell, and M. Neubert, Phys.Lett. **B704**, 276 (2011), 15 pages, 4 figures, arXiv:1104.4108 [hep-ph].

[28] J.-Y. Chiu, A. Jain, D. Neill, and I. Z. Rothstein, JHEP **1205**, 084 (2012), arXiv:1202.0814 [hep-ph].

[29] R. Abbate, M. Fickinger, A. H. Hoang, V. Mateu, and I. W. Stewart, Phys. Rev. **D86**, 094002 (2012), arXiv:1204.5746 [hep-ph].

[30] R. Abbate, M. Fickinger, A. H. Hoang, V. Mateu, and I. W. Stewart, Phys. Rev. **D83**, 074021 (2011), arXiv:1006.3080.

[31] W. Bernreuther, A. Brandenburg, and P. Uwer, Phys.Rev.Lett. **79**, 189 (1997), arXiv:hep-ph/9703305 [hep-ph].

[32] G. Rodrigo, M. S. Bilenky, and A. Santamaria, Nucl. Phys. **B554**, 257 (1999), arXiv:hep-ph/9905276.

[33] A. Brandenburg and P. Uwer, Nucl. Phys. **B515**, 279 (1998), arXiv:hep-ph/9708350.

[34] S. Fleming, A. H. Hoang, S. Mantry, and I. W. Stewart, Phys. Rev. **D77**, 074010 (2008), arXiv:hep-ph/0703207.

[35] S. Fleming, A. H. Hoang, S. Mantry, and I. W. Stewart, Phys. Rev. **D77**, 114003 (2008), arXiv:0711.2079 [hep-ph].

[36] Y. L. Dokshitzer and B. R. Webber, Phys. Lett. **B352**, 451 (1995), arXiv:hep-ph/9504219.

[37] Y. L. Dokshitzer, G. Marchesini, and B. R. Webber, Nucl. Phys. **B469**, 93 (1996), arXiv:hep-ph/9512336.

[38] Y. L. Dokshitzer, A. Lucenti, G. Marchesini, and G. Salam, JHEP **9805**, 003 (1998), arXiv:hep-ph/9802381 [hep-ph].

[39] M. Beneke, Phys. Rept. **317**, 1 (1999), hep-ph/9807443.

[40] R. Akhoury and V. I. Zakharov, Phys. Lett. **B357**, 646 (1995), arXiv:hep-ph/9504248.

[41] R. Akhoury and V. I. Zakharov, Nucl.Phys. **B465**, 295 (1996), arXiv:hep-ph/9507253 [hep-ph].

[42] P. Nason and M. H. Seymour, Nucl. Phys. **B454**, 291 (1995), arXiv:hep-ph/9506317.

[43] M. Beneke and V. M. Braun, Nucl.Phys.Proc.Suppl. **51C**, 217 (1996), arXiv:hep-ph/9605375 [hep-ph].

[44] G. P. Korchemsky and G. Sterman, Nucl. Phys. **B437**, 415 (1995), arXiv:hep-ph/9411211.

[45] Y. L. Dokshitzer, A. Lucenti, G. Marchesini, and G. Salam, Nucl.Phys. **B511**, 396 (1998), arXiv:hep-ph/9707532 [hep-ph].

[46] E. Gardi and G. Grunberg, JHEP **9911**, 016 (1999), arXiv:hep-ph/9908458 [hep-ph].

[47] E. Gardi and J. Rathsman, Nucl. Phys. **B609**, 123 (2001), arXiv:hep-ph/0103217.

[48] E. Gardi and J. Rathsman, Nucl. Phys. **B638**, 243 (2002), arXiv:hep-ph/0201019.

[49] A. Heister *et al.* (ALEPH), Eur. Phys. J. **C35**, 457 (2004).

[50] C. W. Bauer, A. V. Manohar, and M. B. Wise, Phys. Rev. Lett. **91**, 122001 (2003), arXiv:hep-ph/0212255.

[51] P. Achard *et al.* (L3), Phys. Rept. **399**, 71 (2004), arXiv:hep-ex/0406049.

[52] G. P. Korchemsky and S. Tafat, JHEP **10**, 010 (2000), arXiv:hep-ph/0007005.

[53] T. Gehrmann, M. Jaquier, and G. Luisoni, Eur. Phys. J. **C67**, 57 (2010), arXiv:0911.2422 [Unknown].

[54] G. P. Korchemsky and G. Sterman, Nucl. Phys. **B555**, 335 (1999), arXiv:hep-ph/9902341.

[55] J. C. Collins and D. E. Soper, Nucl. Phys. **B193**, 381 (1981).

[56] G. P. Korchemsky, (1998), arXiv:hep-ph/9806537.

[57] C. W. Bauer, S. Fleming, and M. E. Luke, Phys. Rev. D **63**, 014006 (2001), hep-ph/0005275.

[58] C. W. Bauer, S. Fleming, D. Pirjol, and I. W. Stewart, Phys. Rev. D **63**, 114020 (2001), hep-ph/0011336.

[59] C. W. Bauer and I. W. Stewart, Phys. Lett. B **516**, 134 (2001), hep-ph/0107001.

[60] C. W. Bauer, D. Pirjol, and I. W. Stewart, Phys. Rev. **D65**, 054022 (2002), arXiv:hep-ph/0109045.

[61] C. W. Bauer, S. Fleming, D. Pirjol, I. Z. Rothstein, and I. W. Stewart, Phys. Rev. D **66**, 014017 (2002), hep-ph/0202088.

[62] A. H. Hoang and I. W. Stewart, Phys. Lett. **B660**, 483 (2008), arXiv:0709.3519 [hep-ph].

[63] Z. Ligeti, I. W. Stewart, and F. J. Tackmann, Phys. Rev. **D78**, 114014 (2008), arXiv:0807.1926 [hep-ph].

[64] A. H. Hoang, A. Jain, I. Scimemi, and I. W. Stewart, Phys. Rev. Lett. **101**, 151602 (2008), arXiv:0803.4214 [hep-ph].

[65] A. H. Hoang, A. Jain, I. Scimemi, and I. W. Stewart, Phys.Rev. **D82**, 011501 (2010), arXiv:0908.3189 [hep-ph].

[66] N. Sveshnikov and F. Tkachov, Phys.Lett. **B382**, 403 (1996), arXiv:hep-ph/9512370 [hep-ph].

[67] G. P. Korchemsky, G. Oderda, and G. Sterman, "Power Corrections and Nonlocal Operators," (1997), arXiv:hep-ph/9708346v1 [hep-ph].

[68] C. W. Bauer, S. P. Fleming, C. Lee, and G. F. Sterman, Phys.Rev. **D78**, 034027 (2008), arXiv:0801.4569 [hep-ph].

[69] I. W. Stewart, F. J. Tackmann, and W. J. Waalewijn, Phys.Rev.Lett. **105**, 092002 (2010), arXiv:1004.2489 [hep-ph].

[70] G. C. Fox and S. Wolfram, Phys.Rev.Lett. **41**, 1581 (1978).

[71] G. C. Fox and S. Wolfram, Nucl.Phys. **B149**, 413 (1979).

[72] S. Catani, G. Turnock, and B. Webber, Phys.Lett. **B295**, 269 (1992).

[73] F. V. Tkachov, Int.J.Mod.Phys. **A17**, 2783 (2002), arXiv:hep-ph/9901444 [hep-ph].

[74] A. V. Belitsky, G. P. Korchemsky, and G. Sterman, Phys. Lett. **B515**, 297 (2001), arXiv:hep-ph/0106308.

[75] C. F. Berger and G. Sterman, JHEP **09**, 058 (2003), arXiv:hep-ph/0307394.

[76] C. F. Berger and L. Magnea, Phys.Rev. **D70**, 094010 (2004), arXiv:hep-ph/0407024 [hep-ph].

[77] E. Gardi, JHEP **0004**, 030 (2000), arXiv:hep-ph/0003179 [hep-ph].

[78] A. H. Hoang and S. Kluth, (2008), arXiv:0806.3852 [hep-ph].

[79] A. Jain, I. Scimemi, and I. W. Stewart, Phys. Rev. **D77**, 094008 (2008), arXiv:0801.0743 [hep-ph].

[80] Y. L. Dokshitzer, Sov.Phys.JETP **46**, 641 (1977).

[81] V. Gribov and L. Lipatov, Sov.J.Nucl.Phys. **15**, 438 (1972).

[82] G. Altarelli and G. Parisi, Nucl.Phys. **B126**, 298 (1977).

[83] T. Sjostrand, S. Mrenna, and P. Skands, Comput.Phys.Commun.178:852-867,2008 (2007), 10.1016/j.cpc.2008.01.036, arXiv:0710.3820v1 [hep-ph].

[84] M. Bahr, S. Gieseke, M. A. Gigg, D. Grellscheid, K. Hamilton, O. Latunde-Dada, S. Platzer, P. Richardson, M. H. Seymour, A. Sherstnev, J. Tully, and B. R. Webber, Eur.Phys.J.C58:639-707,2008 (2008), 10.1140/epjc, arXiv:0803.0883v3 [hep-ph].

[85] A. G. Holzner, R. Gokieli, P. Igo-Kemenes, M. Maggi, L. Malgeri, *et al.*, (2009), arXiv:0912.1803 [hep-ex].

[86] Z. Akopov *et al.* (DPHEP Study Group), (2012), arXiv:1205.4667 [hep-ex].

[87] J. Thaler and K. Van Tilburg, JHEP **1103**, 015 (2011), arXiv:1011.2268 [hep-ph].

[88] J. Thaler and K. Van Tilburg, JHEP **1202**, 093 (2012), arXiv:1108.2701 [hep-ph].

[89] J.-H. Kim, Phys.Rev. **D83**, 011502 (2011), arXiv:1011.1493 [hep-ph].

[90] I. Feige, M. Schwartz, I. Stewart, and J. Thaler, Phys.Rev.Lett. **109**, 092001 (2012), arXiv:1204.3898 [hep-ph].

[91] J. G. M. Gatheral, Phys. Lett. **B133**, 90 (1983).

[92] J. Frenkel and J. C. Taylor, Nucl. Phys. **B246**, 231 (1984).

[93] R. Kelley, M. D. Schwartz, R. M. Schabinger, and H. X. Zhu, Phys.Rev. **D84**, 045022 (2011), arXiv:1105.3676 [hep-ph].

[94] A. Hornig, C. Lee, I. W. Stewart, J. R. Walsh, and S. Zuberi, JHEP **1108**, 054 (2011), arXiv:1105.4628 [hep-ph].

[95] P. F. Monni, T. Gehrmann, and G. Luisoni, JHEP **1108**, 010 (2011), arXiv:1105.4560 [hep-ph].